AD-A046 411 NAVAL UNDERWATER SYSTEMS CENTER NEW LONDON CONN NEW --ETC F/G 9/5
RESULTS OF THE WISCONSIN TEST FACILITY PHASING ANOMALY INVESTIG--ETC(U)
SEP 77 P R BANNISTER

UNCLASSIFIED NUSC-TR-5719 NL

1 OF 1
AD A046411

END
DATE FILMED
12-77
DDC

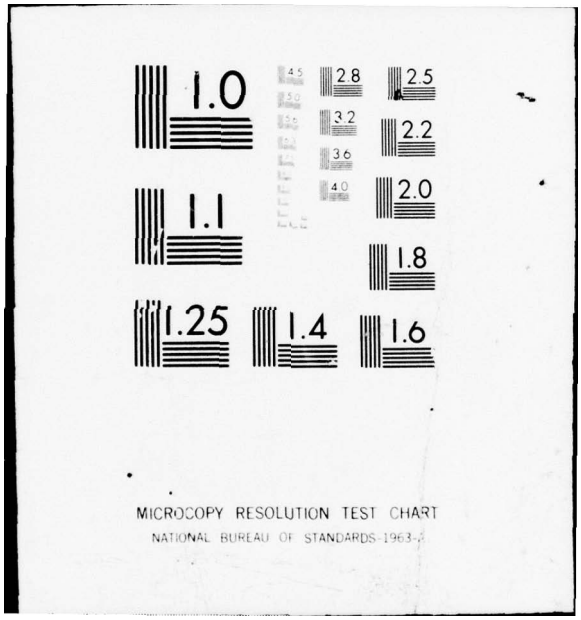
1.0
1.1
1.25
1.4
1.6
1.8
2.0
2.2
2.5
2.8
3.2
3.6
4.0
4.5
5.0
5.6
MICROCOPY RESOLUTION TEST CHART
NATIONAL BUREAU OF STANDARDS-1963-A

12

Results of the Wisconsin Test Facility Phasing Anomaly Investigations

Peter R. Bannister
Submarine Electromagnetic Systems Department

29 September 1977

NUSC

NAVAL UNDERWATER SYSTEMS CENTER
Newport, Rhode Island • New London, Connecticut

PREFACE

This research was performed under NUSC Project No. A59007, "Project SEAFARER ELF Propagation Studies" (U), Principal Investigator — P. R. Bannister (Code 341), and Navy Program Element No. 11401 and Project No. X0792, Program Manager — Dr. B. Kruger (NAVELEX, PME-117-21).

The Technical Reviewer for this report was J. J. Tennyson (Code 3403).

REVIEWED AND APPROVED: 29 September 1977

John Merrill

John Merrill
Head: Submarine Electromagnetic Systems Department

The author of this report is located at the New London Laboratory, Naval Underwater Systems Center, New London, Connecticut 06320.

TABLE OF CONTENTS

LIST OF ILLUSTRATIONS

LIST OF ILLUSTRATIONS (Cont'd)

REPORT DOCUMENTATION PAGE

READ INSTRUCTIONS BEFORE COMPLETING FORM

1. REPORT NUMBER: NUSC-TR-5719	2. GOVT ACCESSION NO.
3. RECIPIENT'S CATALOG NUMBER: Technical Rept.	
4. TITLE (and Subtitle): RESULTS OF THE WISCONSIN TEST FACILITY PHASING ANOMALY INVESTIGATIONS.	5. TYPE OF REPORT & PERIOD COVERED
	6. PERFORMING ORG. REPORT NUMBER
7. AUTHOR(s): Peter. R. Bannister	8. CONTRACT OR GRANT NUMBER(s)
9. PERFORMING ORGANIZATION NAME AND ADDRESS: Naval Underwater Systems Center, New London Laboratory, New London, CT 06320	10. PROGRAM ELEMENT, PROJECT, TASK AREA & WORK UNIT NUMBERS: A-590-07, X0792
11. CONTROLLING OFFICE NAME AND ADDRESS: Naval Electronics Systems Command (PME-117), Washington, DC 20360	12. REPORT DATE: 29 September 1977
	13. NUMBER OF PAGES: 46
14. MONITORING AGENCY NAME & ADDRESS(if different from Controlling Office): 12) 48p.	15. SECURITY CLASS. (of this report): UNCLASSIFIED
	15a. DECLASSIFICATION/DOWNGRADING SCHEDULE

16. DISTRIBUTION STATEMENT (of this Report)

Approved for public release; distribution unlimited.

17. DISTRIBUTION STATEMENT (of the abstract entered in Block 20, if different from Report)

18. SUPPLEMENTARY NOTES

19. KEY WORDS (Continue on reverse side if necessary and identify by block number)

Extremely Low Frequency (ELF)	WTF Antenna Array
Phasing Anomalies	WTF Antenna Phasing Shift
Quasi-Orthogonal Antennas	WTF Effective Dipole Moment
Wisconsin Test Facility (WTF)	WTF Pattern Factor

20. ABSTRACT (Continue on reverse side if necessary and identify by block number)

Since 1974, many Wisconsin Test Facility (WTF) phasing anomalies have been observed. Among these anomalies are (1) $\psi°$ phasing does not equal $(360°-\psi°)$, contrary to the normal behavior of crossed dipoles; (2) the maximum field strength at any single receiving location is not when $\psi = 0°$ or $180°$; (3) the WTF antenna phasing shift appears to be $-20°$ to $-30°$; (4) the WTF effective dipole moment does not appear to be independent of ψ; and (5) the WTF antenna phasing shift appears to be a function of azimuth angle. By → (over)

DD FORM 1 JAN 73 1473

405 918

20. ABSTRACT (Con't)

a combination of nearfield and farfield measurements, we have empirically determined a new WTF pattern factor that quantitatively explains these anomalies.

RESULTS OF THE WISCONSIN TEST FACILITY PHASING ANOMALY INVESTIGATIONS

INTRODUCTION

The U. S. Navy's extremely low frequency (ELF) Wisconsin Test Facility (WTF) is located in the Chequamegon National Forest in north-central Wisconsin, about 8 km south of the village of Clam Lake. The WTF consists of two 22.5 km quasi-orthogonal antennas (NS, EW), with the transmitting station at the midpoints of the antennas. Each antenna is grounded at both ends. It should be noted that the antenna lines are not straight; i.e., the general direction is 19°E of N for the NS antenna and 109°E of N for the EW antenna. The WTF antenna array can be steered to any particular direction and its radiated power is approximately 1 W.

During August and September of 1971, pattern and steering measurements[1,2] were performed on the NS and EW antennas of the WTF. The pattern measurements were made at 13 different locations 300 km distant in eastern Minnesota and southern Wisconsin (covering approximately 120° of arc); the farfield (1.7 Mm) steering measurements were made in Mars Hill, Maine, and Swansboro, North Carolina. It was learned from the pattern and steering measurements that the EW antenna pattern is skewed clockwise, and the NS antenna pattern is skewed counterclockwise. The electrical axis of the WTF EW antenna is 118°E of N at 45 Hz and 114°E of N at 75 Hz; the electrical axis of the WTF NS antenna is 11°E of N at 45 Hz and 14°E of N at 75 Hz.[1,2]

From 1971 until about March 1974, the WTF performed as predicted when different phasings were employed. However, after that time, many phasing anomalies were observed. In this report we will discuss these anomalies and introduce a new WTF pattern factor that quantitatively explains them.

OLD WTF PATTERN FACTOR

From figure 1 we see that the steered pattern factor $F(\phi)$ for the H_ϕ component, produced by an unorthogonal array composed of two horizontal electric-transmitting antennas, may be expressed as[1,2]

$$F(\phi) = A \cos \phi + B \cos(\phi - \theta) \exp(j\psi) \quad , \tag{1}$$

where

ϕ is the azimuth angle with respect to the NS antenna,

$(\phi - \theta)$ is the azimuth angle with respect to the EW antenna,

θ is the electrical angle between the NS and EW antennas,

ψ is the phasing angle between the antennas (ψ is set up at the transmitting station),

A is the maximum field strength produced by the NS antenna, and

B is the maximum field strength produced by the EW antenna.

Note that[1,2]

$$\frac{A}{B} = \frac{I_{NS} L_{NS}}{I_{EW} L_{EW}} \left(\frac{\sigma_{eEW}}{\sigma_{eNS}} \right)^{\frac{1}{2}} \quad , \tag{2}$$

where σ_e is the effective earth conductivity beneath the transmitting antenna. Thus, when both antennas are of equal length and current,

$$\frac{A}{B} = \sqrt{\frac{\sigma_{eEW}}{\sigma_{eNS}}} \quad . \tag{3}$$

At 75 Hz, A/B = 1.20 and $\theta = 100^\circ$, while at 45 Hz, A/B = 1.30 and $\theta = 107^\circ$.[1,2,3]

The magnitude of $F(\phi)$ may be written as

$$|F(\phi)| = [A^2 \cos^2 \phi + 2AB \cos \phi \cos(\phi - \theta) \cos \psi + B^2 \cos^2(\phi - \theta)]^{\frac{1}{2}} \quad . \tag{4}$$

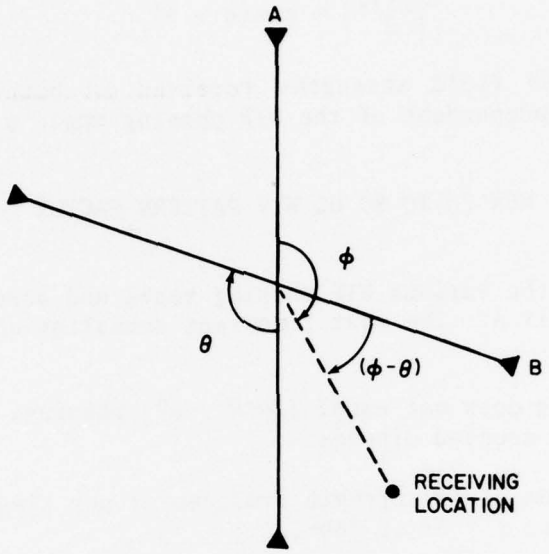

Figure 1. Unorthogonal Array Diagram of Two Horizontal Electric Transmitting Antennas

If A = B = 1 and $\psi = 180^{o} - \theta$, then $F(\phi) = \sin\theta$. For this case, $F(\phi)$ is independent of ϕ and an omnidirectional pattern with a normalized amplitude of $\sin\theta$ is realized.

If the WTF EW antenna is used as the reference for defining the WTF antenna pattern factor, equation (4) becomes

$$\left|\frac{F(\phi)}{B}\right| = \frac{A}{B}\left[\cos^2\phi + \frac{2\cos\phi\cos(\phi-\theta)\cos\psi}{(A/B)} + \frac{\cos^2(\phi-\theta)}{(A/B)^2}\right]^{\frac{1}{2}} . \quad (5)$$

Referring to equation (5), we see that the maximum field strength produced at any single location is realized when $\psi = 0$ or 180^{o}. Furthermore, since $\cos\psi = \cos(360^{o} - \psi)$, the field strengths received at 60^{o} and 300^{o} phasing should be identical.

When $(\phi - \theta) \sim \pi/2$ or $3\pi/2$ (i.e., Tromsö, Norway, at 75 Hz)

$$\left|\frac{F(\phi)}{B}\right| \sim \frac{A}{B}\cos\phi \quad , \quad (6)$$

and, when $\phi \sim \pi/2$ or $3\pi/2$ (i.e., New London, Connecticut, at 75 Hz)

$$\left|\frac{F(\phi)}{B}\right| \sim \cos(\phi - \theta) \quad . \tag{7}$$

Thus, at 75 Hz the field strengths received in both New London and Tromsö should be independent of the WTF phasing angle ψ.

NEW 70 TO 80 HZ WTF PATTERN FACTOR

A history of the various WTF phasing tests and observed anomalies is given in appendix A. The most important anomalies observed to date are

1. ψ^o phasing does not equal $(360^o - \psi^o)$ phasing, contrary to the normal behavior of crossed dipoles.

2. The maximum field strength produced at any single receiving location is not when $\psi = 0^o$ or 180^o.

3. The H_ϕ field strengths received in New London (which is broadside to the WTF NS antenna) and in Tromsö (which is broadside to the WTF EW antenna) are no longer independent of ψ at 75 Hz.

4. The WTF antenna phasing shift appears to be -20^o to -30^o (i.e., when the antennas are set up at 60^o phasing, the actual phasing is 30^o to 40^o).

5. The WTF effective dipole moment does not appear to be constant with phasing angle ψ. At 75 Hz, the NS antenna effective dipole moment appears to vary as $[1 + 0.12 \sin(\psi - 20^o)]$, whereas the EW antenna effective dipole moment appears to vary as $[1 - 0.12 \sin(\psi - 20^o)]$.

6. The WTF antenna phasing shift appears to be a function of receiver location (i.e., azimuth angle).

Many of the observed phasing anomalies appear to be contradictory. However, they can be explained quantitatively by a simple modification to the old WTF pattern factor (equation (5)).

Based on a combination of nearfield and farfield measurements (see appendixes A and B), we have determined empirically that, in the 70 to 80 Hz band, the new WTF pattern factor for the H_ϕ component is of the form

$$F(\phi) \sim k_1 A \cos\phi + k_2 B \cos(\phi - \theta) e^{j(\psi - 20^o)} \quad , \tag{8}$$

where

$k_1 = 1 + 0.12 \sin(\psi - 20^o)$,

$k_2 = 1 - 0.12 \sin(\psi - 20^o)$,

$A/B = 1.20$, and

$\theta = 100^o$.

Note that the new pattern factor at 20^o and 200^o is identical to the old pattern factor at 0^o and 180^o.

The magnitude of $F(\phi)$ may be written as

$$|F(\phi)| \sim \left[k_1^2 A^2 \cos^2\phi + 2ABk_1k_2 \cos\phi \cos(\phi - \theta) \cos(\psi - 20^o) + k_2^2 B^2 \cos^2(\phi - \theta)\right]^{\frac{1}{2}} \quad . \tag{9}$$

If the WTF EW antenna is used as the reference for defining the new WTF antenna pattern factor, equation (9) becomes

$$\left|\frac{F(\phi)}{B}\right| \sim \frac{A}{B}\left\{k_1^2 \cos^2\phi + \frac{2k_1k_2 \cos\phi \cos(\phi - \theta) \cos(\psi - 20^o)}{(A/B)} + \frac{k_2^2 \cos^2(\phi - \theta)}{(A/B)^2}\right\}^{\frac{1}{2}} \quad . \tag{10}$$

Referring to equation (10), we see that the maximum field strength produced at any single location is not realized when $\psi = 0^o$ or 180^o. Furthermore, the field strengths received at 60^o and 300^o phasing will not be identical.

When $(\phi - \theta) \sim \pi/2$ or $3\pi/2$ (i.e., Tromsö),

$$\left|\frac{F(\phi)}{B}\right| \sim k_1 \frac{A}{B} \cos\phi \approx [1 + 0.12 \sin(\psi - 20^o)] \frac{A}{B} \cos\phi \quad , \tag{11}$$

and, when $\phi \sim \pi/2$ or $3\pi/2$ (i.e., New London),

$$\left|\frac{F(\phi)}{B}\right| \sim k_2 \cos(\phi - \theta) \approx [1 - 0.12 \sin(\psi - 20^o)] \cos(\phi - \theta) \quad . \tag{12}$$

Thus, in the 70 to 80 Hz band, the field strengths received in both New London and Tromsö are not independent of the WTF phasing angle ψ.

It can be shown that, under some conditions, the new WTF pattern factor is approximately equivalent to

$$F(\phi) \sim A \cos \phi + B \cos(\phi - \theta) e^{j(\psi - \Delta)} \quad , \tag{13}$$

where

$$|F(\phi)| \sim [A^2 \cos^2 \phi + 2AB \cos \phi \cos(\phi - \theta) \cos(\psi - \Delta) + B^2 \cos^2(\phi - \theta)]^{\frac{1}{2}} \quad , \tag{14}$$

and Δ is a function of receiver location (i.e., azimuth angle). That is, the new equivalent WTF pattern factor (equation (13)) is very similar to the old WTF pattern factor (equation (1)), except that $(\psi - \Delta)^o$ is substituted for ψ^o at each receiving site.

Equating equations (9) and (14) and solving for Δ results in

$$\Delta \approx 110^o - \cos^{-1}\left\{\frac{(k_1^2 - 1)(A/B)\cos \phi}{2 \cos(\phi - \theta)} + \frac{(k_2^2 - 1)\cos(\phi - \theta)}{2(A/B)\cos \phi}\right\} \quad . \tag{15}$$

This equation will not be valid for ϕ or $(\phi - \theta)$ between $n\pi/2 - 10^o$ and $n\pi/2 + 10^o$ (n odd).

In figure 2, Δ is plotted versus ϕ and $\phi - \theta$, and we see that for Stumpneck, Maryland ($\phi \sim 107^o$), $\Delta \sim 35^o$, while for Casco ($\phi \sim 77^o$), $\Delta \sim 0^o$.

The new WTF pattern factor (equation (10)) quantitatively explains most of the observed phasing anomalies; that is,

1. it shows that ψ^o phasing does not equal $(360^o - \psi^o)$ phasing;

2. it shows that the maximum field strength produced at any single receiving location is not realized when $\psi = 0^o$ or 180^o;

3. it shows that the H_ϕ field strengths received in New London and Tromsö are no longer independent of ψ;

4. it accounts for a -20^o phase shift;

5. it accounts for a change in effective dipole moment of both WTF antennas; and

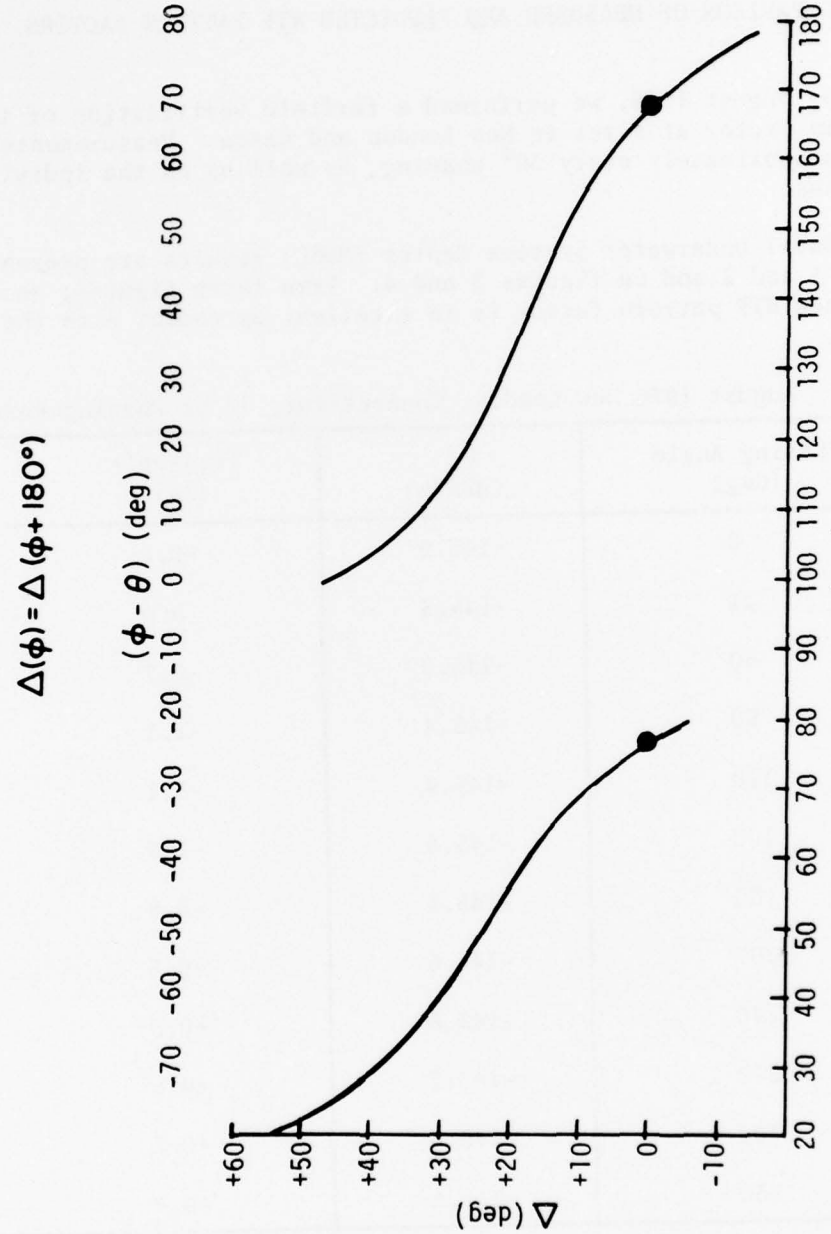

Figure 2. Δ Versus φ and (φ - θ) for f = 70 to 80 Hz, A/B = 1.20, and θ = 100°

6. it shows that the phase shift observed can be a function of receiver location.

COMPARISON OF MEASURED AND PREDICTED WTF PATTERN FACTORS

During August 1976, we performed a farfield verification of the new WTF pattern factor at sites in New London and Casco. Measurements were taken at approximately every 30^{o} phasing, as well as on the individual WTF antennas.

The Naval Underwater Systems Center (NUSC) results are presented in tables 1 and 2 and in figures 3 and 4. From these figures, we see that the new WTF pattern factor is in excellent agreement with the measured data.

Table 1. August 1976 New London, Connecticut, 72 Hz Phasing Results

Phasing Angle (deg)	H_{ϕ} (dBA/m)	$\lvert F(\phi)/B \rvert$* (dB)
0	-143.9	+0.4
21	-144.3	0.0
60	-145.0	-0.7
90	-145.4	-1.1
110	-145.4	-1.1
120	-145.8	-1.5
180	-145.1	-0.8
207	-144.6	-0.3
240	-143.8	+0.5
270	-143.7	+0.6
300	-143.6	+0.7
330	-143.6	+0.7

*Reference H_{ϕ} = -144.3 dBA/m.

Table 2. August 1976 Casco, Maine, 72 Hz Phasing Results

Phasing Angle (deg)	H_ϕ (dBA/m)	$\lvert F(\phi)/B \rvert$* (dB)
0	-142.8	+1.55
21	-143.0	+1.35
60	-143.7	+0.65
90	-144.7	-0.35
120	-146.1	-1.75
150	-147.6	-3.25
180	-148.4	-4.05
200	-148.0	-3.65
222	-146.9	-2.55
240	-145.7	-1.35
270	-144.5	-0.15
300	-143.4	+0.95
330	-143.1	+1.25
EW	-145.0	-0.65
NS	-156.0	-11.65

*Reference H_ϕ = -144.35 dBA/m.

The Naval Research Laboratory (NRL) also measured WTF field strengths during August 1976 in Stumpneck and Tromsö. Their results[4] are presented in figures 5 and 6. The average values of the 1975 Stumpneck measurements also are included. The solid-line curve in each figure is calculated from the old WTF pattern factor (equation (5)), while the dashed-line curve is calculated from the new WTF pattern factor (equation (10)). From these figures, we see that equation (10) also is an excellent approximation to the pattern factors for Tromsö and Stumpneck. There is much more scatter in the Tromsö data, but this is to be expected since the signal-to-noise ratio (SNR) is lower there.

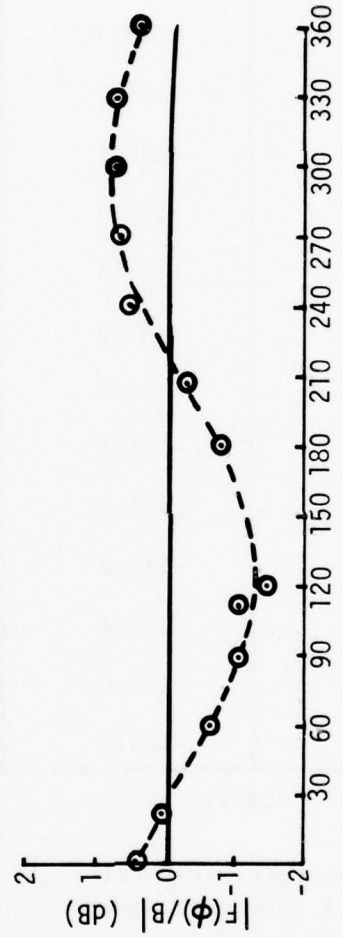

Figure 3. 72 Hz Comparison of Measured Data With WTF Pattern Factors for New London, Connecticut (0 dB = -144.3 dBA/m)

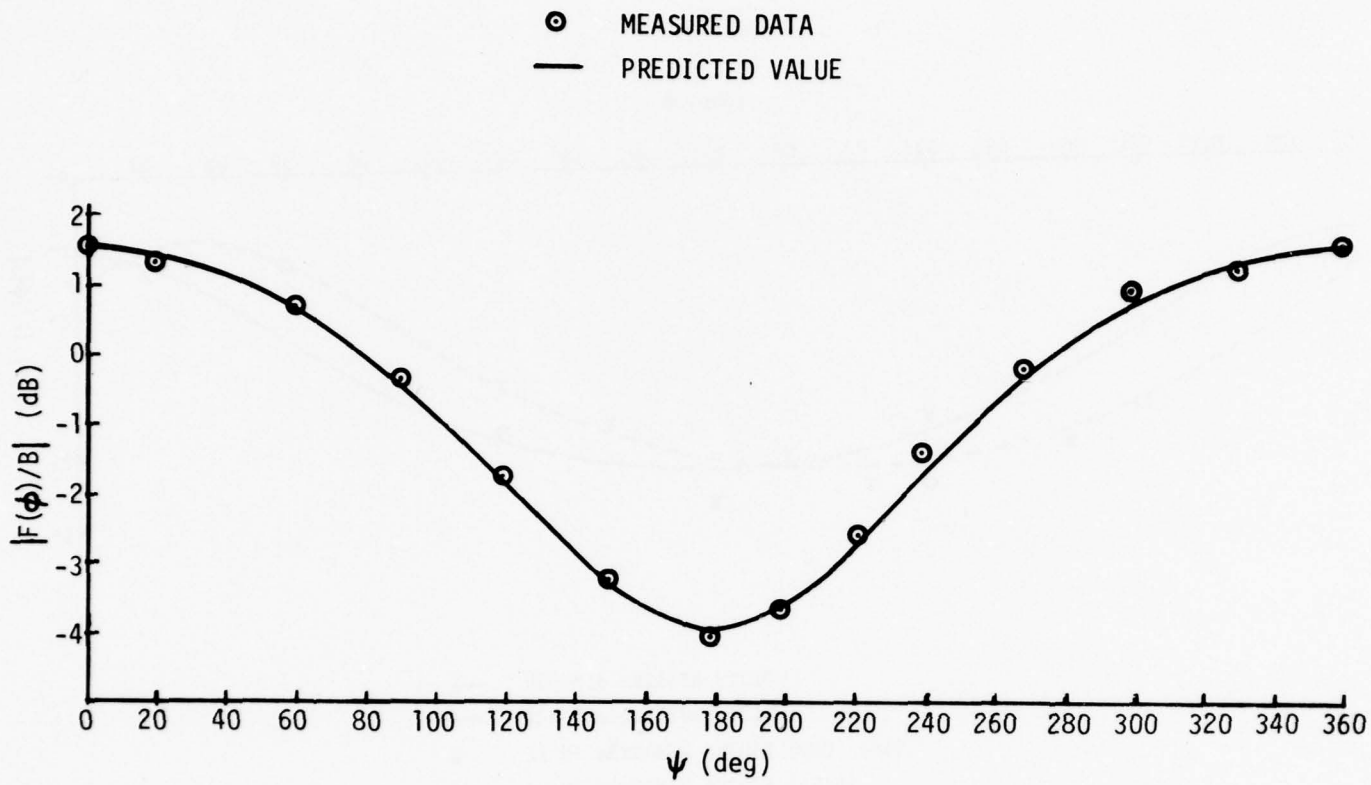

Figure 4. 72 Hz Comparison of Measured Data With New WTF Pattern Factor for Casco, Maine (0 dB = -144.35 dBA/m, $\Delta \sim 0^{o}$)

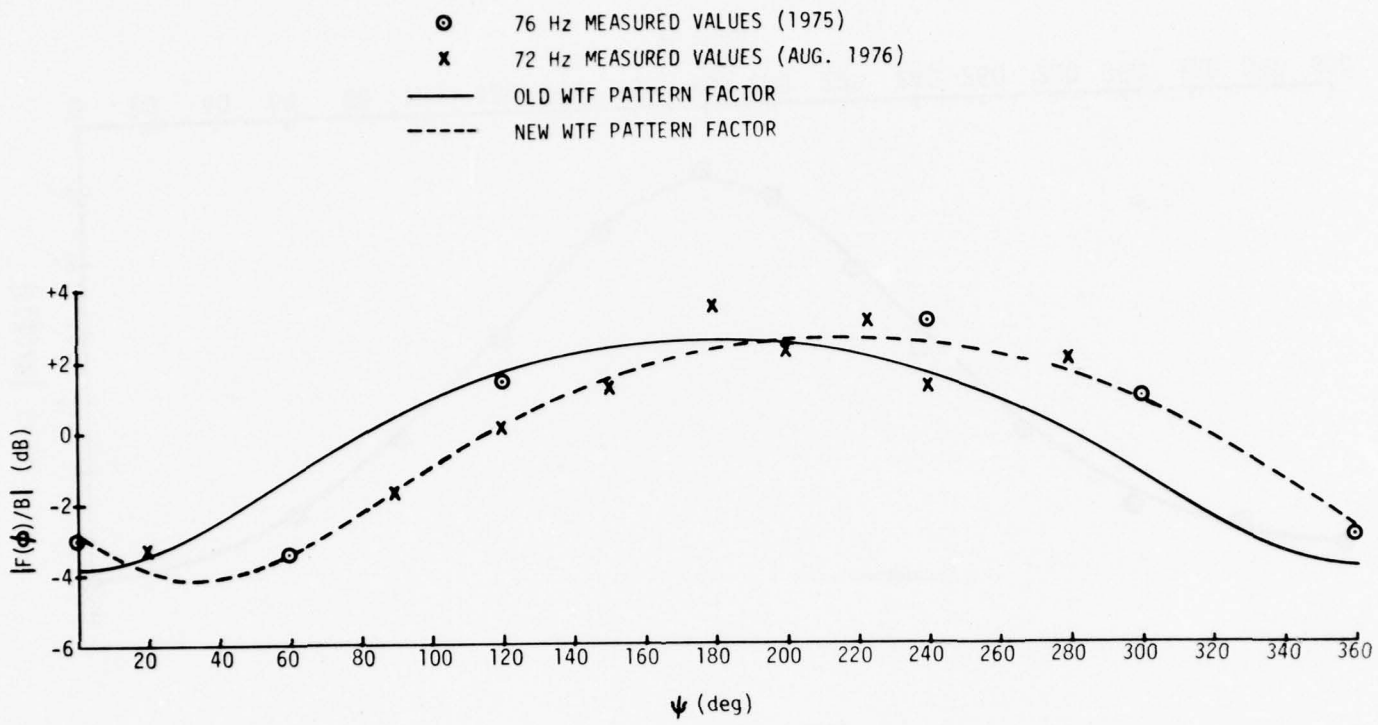

Figure 5. 70 to 80 Hz Band Comparison of Measured Data With WTF Pattern Factors for Stumpneck, Maryland (0 dB = -143.6 dBA/m, $\Delta \sim 35^{o}$)

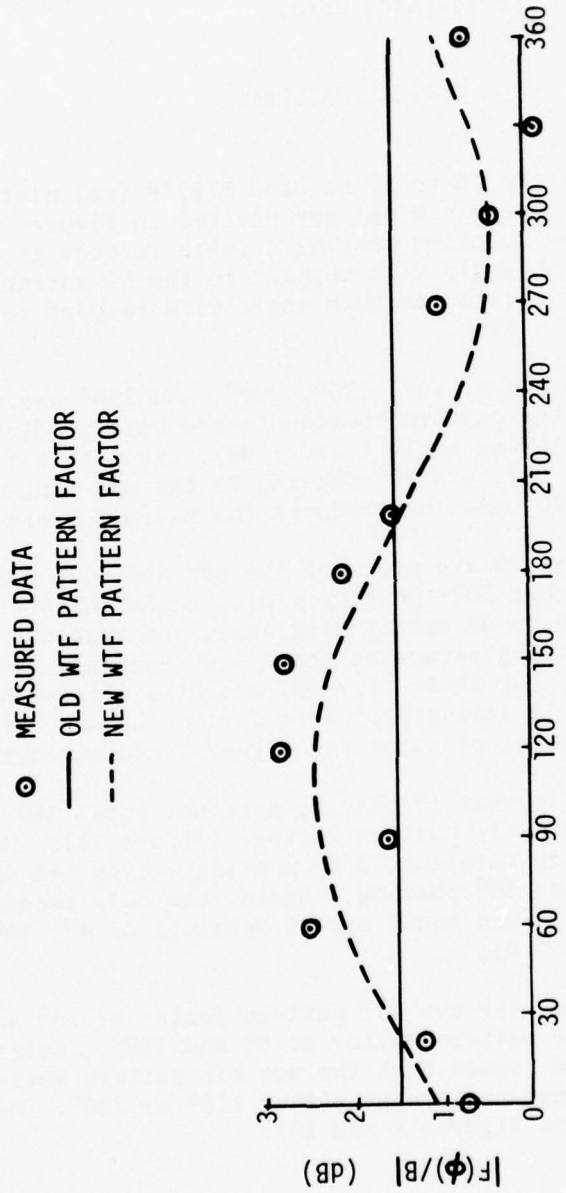

Figure 6. 72 Hz Comparison of Measured Data With WTF Pattern Factors for Tromsö, Norway (0 dB = -154.6 dBA/m)

Presented in figures 7 and 8 are the average values of the 1975 Swansboro, North Carolina, and Thule, Greenland, measurements. The solid-line curve in each figure is calculated from equation (5), while the dashed-line curve is calculated from the new WTF pattern factor (equation (10)). Here, again, we see that the new WTF pattern factor is in good agreement with the measured data.

TYPICAL PATTERNS

Various values of the 70 to 80 Hz band $F(\phi)/B$ (calculated from equation (10), with B = unity = 0 dB) are plotted in figures 9, 10, and 11 versus the receiving location bearing ξ (with respect to true north). Note that ϕ, the azimuth angle with respect to the NS antenna, is equal to $\xi - 14^{o}$, while $(\phi - \theta)$, the azimuth angle with respect to the EW antenna, is equal to $\xi - 114^{o}$.

In figure 9, phasings of 20^{o}, 110^{o}, 200^{o}, and 290^{o} are considered. The outer envelope of the pattern represents the best predicted steering possible for a given bearing angle ξ (±0.1 dB). From this figure, we see that for $32^{o} \leq \xi \leq 98^{o}$, $\psi = 20^{o}$ phasing is the optimum, whereas if $110^{o} \leq \xi \leq 195^{o}$, $\bar{\psi} = \bar{2}00^{o}$ phasing produces the maximum field strength.

Presented in figure 10 are plots of the 60^{o} and 300^{o} WTF pattern factors. Here we see that 300^{o} phasing yields an omnidirectional pattern (i.e., $F(\phi)/B = 0.60 \pm 0.25$ dB at all bearings), and that 60^{o} phasing does not equal 300^{o} phasing except at the $\Delta \sim 0^{o}$ bearings (4^{o}, 90^{o}, 184^{o}, and 270^{o}). Also, for Thule, Tromsö, and Pisa, Italy, 60^{o} phasing produces the higher field strengths, while for New London, Stumpneck, and Swansboro 300^{o} phasing produces the higher field strengths.

As a further example that ψ^{o} phasing does not equal $360 - \psi^{o}$ phasing, consider the 30^{o} and 330^{o} WTF pattern factors (figure 11). Here we see that at Charleston, South Carolina, 330^{o} phasing yields ~10 dB greater field strengths than does 30^{o} phasing. Again, the only locations where the 30^{o} and 330^{o} phasings are equal are at bearings of 4^{o}, 90^{o}, 184^{o}, and 270^{o} (i.e., where $\Delta \sim 0$).

As previously noted, the new WTF pattern factor at 20^{o} and 200^{o} is identical to the old WTF pattern factor at 0^{o} and 180^{o}. Referring to equation (10), one would assume that the new WTF pattern factor would produce an omnidirectional pattern at either 110^{o} or 290^{o}. However, this is not the case (see figures 9 and 10).

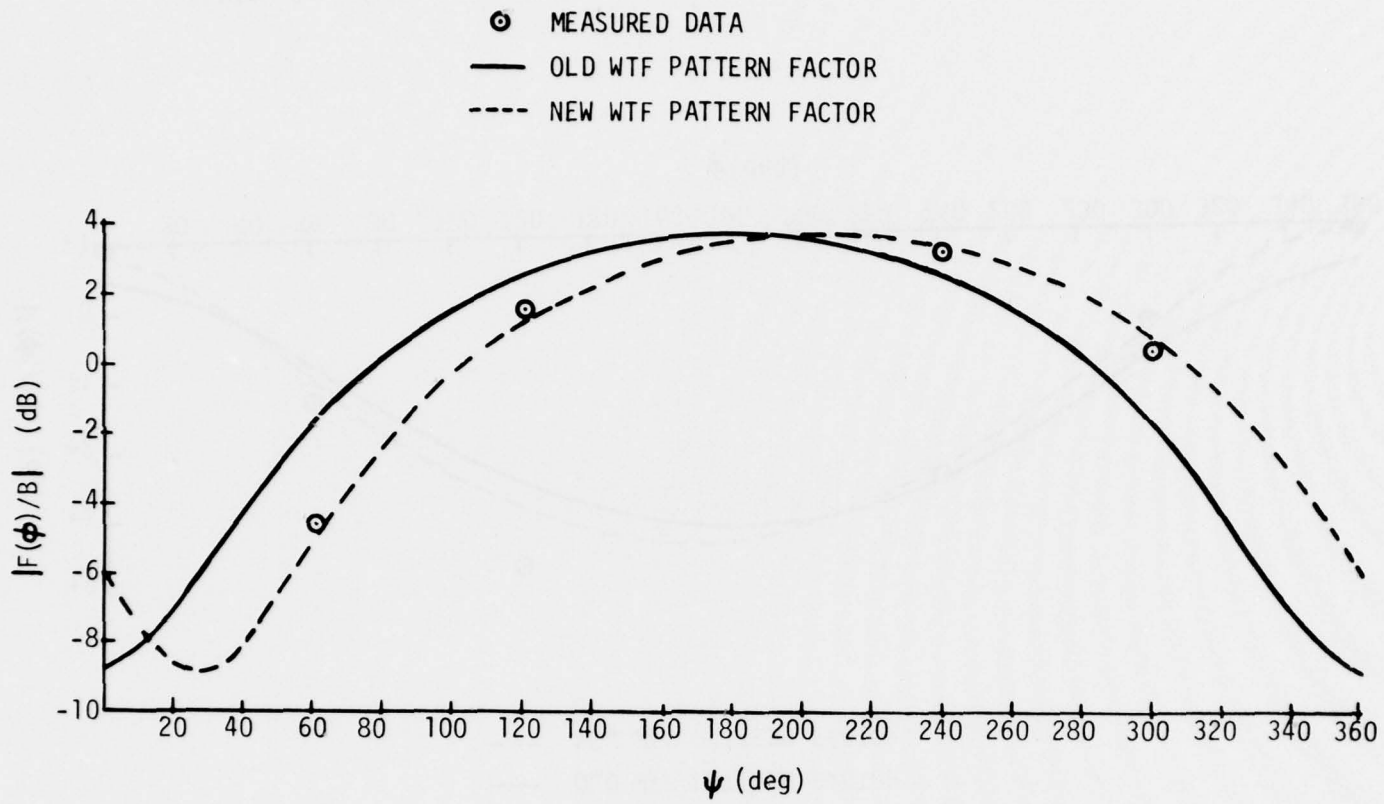

Figure 7. 76 Hz Comparison of Measured Data With WTF Pattern Factors for Swansboro, North Carolina (0 dB = -144.1 dBA/m, $\Delta \sim 25^{o}$)

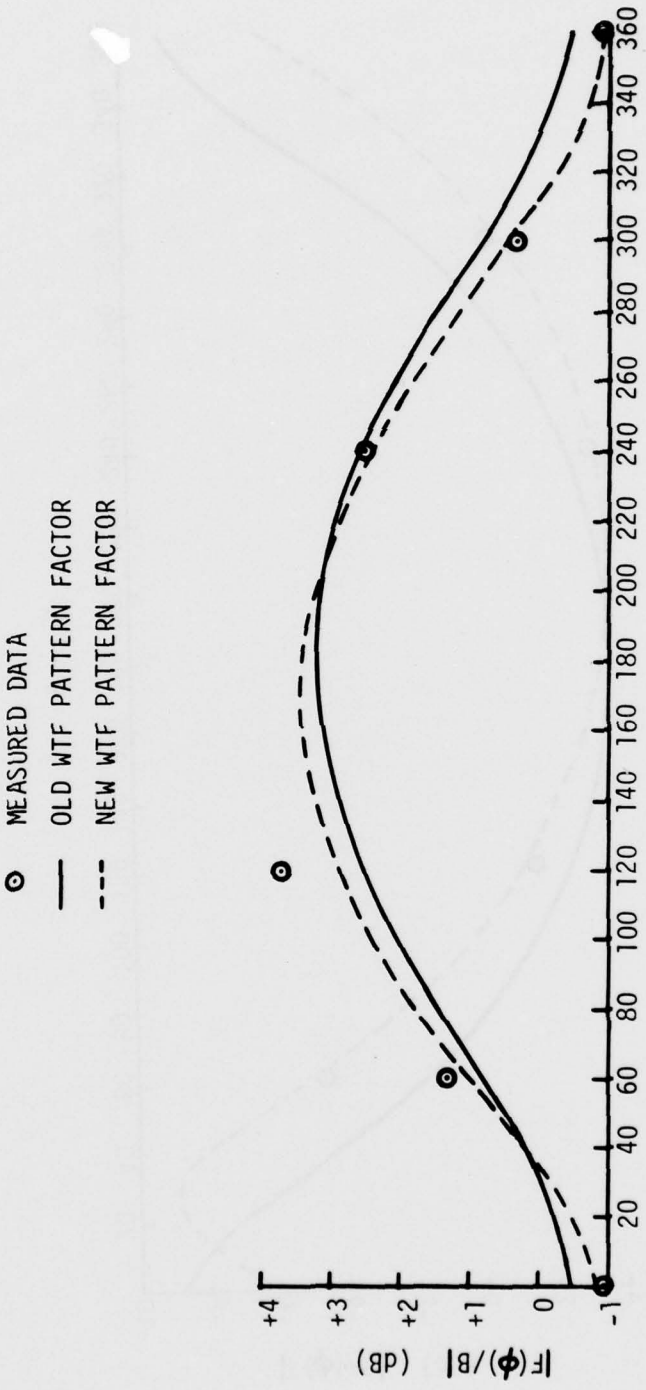

Figure 8. 76 Hz Comparison of Measured Data With WTF Pattern Factors for Thule, Greenland (0 dB = -152.0 dBA/m, $\Delta \sim -10^{0}$)

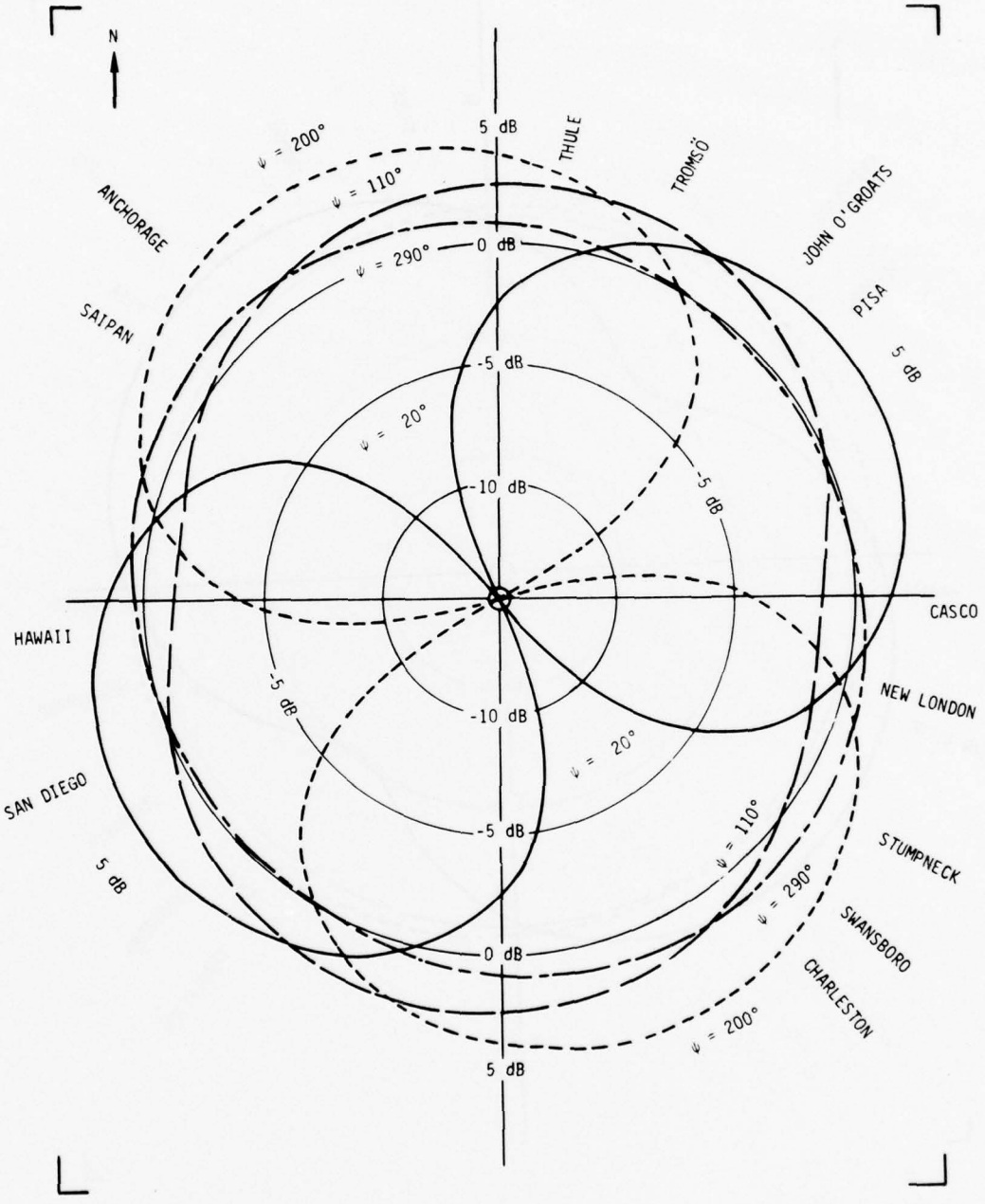

Figure 9. 70 to 80 Hz Band New WTF Pattern Factor Versus Receiving Location Bearing; ψ = 20°, 110°, 200°, and 290°

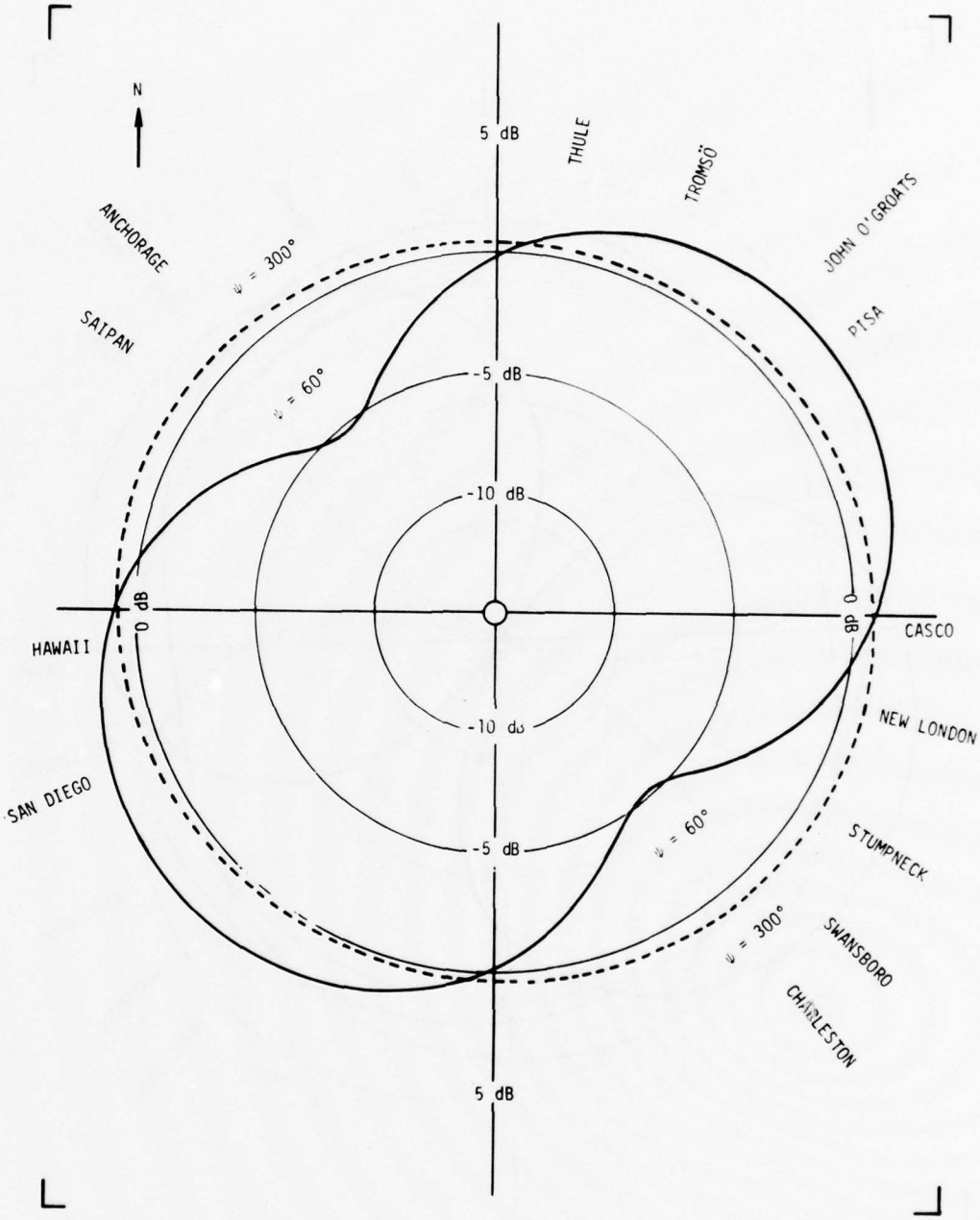

Figure 10. 70 to 80 Hz Band New WTF Pattern Factor Versus Receiving Location Bearing; $\psi = 60^{o}$ and 300^{o}

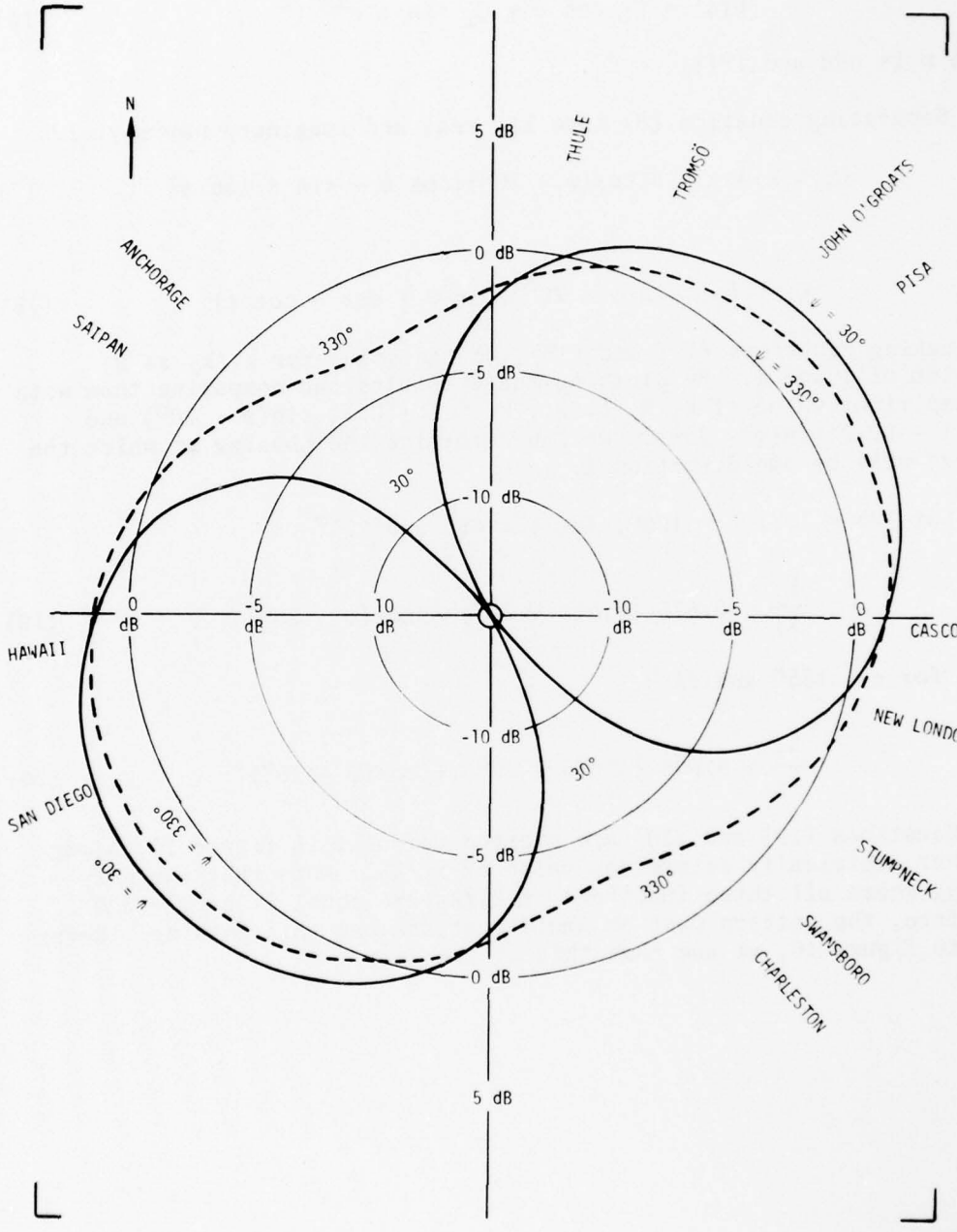

Figure 11. 70 to 80 Hz Band New WTF Pattern Factor Versus Receiving Location Bearing; $\psi = 30^{o}$ and 330^{o}

For the pattern to be omnidirectional,

$$F(\phi) = C_1 \cos \phi + C_1 \sin \phi \, e^{jn\pi/2} \quad , \tag{16}$$

where n is odd and $|F(\phi)| = C_1$.

Separating equation (8) into its real and imaginary parts yields

$$C_1 \sim k_1 A + k_2 B \cos(\psi - 20^o)[\cos \theta + \sin \theta \tan \phi] \quad , \tag{17}$$

and

$$C_2 \sim k_2 B \sin(\psi - 20^o)[\sin \theta + \cos \theta \cot \phi] \quad . \tag{18}$$

By equating equations (17) and (18), we can solve for k_1/k_2 as a function of ϕ and ψ. By plotting these results and comparing them with our empirical value of k_1/k_2 [i.e., $k_1 \sim 1 + 0.12 \sin(\psi - 20^o)$ and $k_2 \sim 1 - 0.12 \sin(\psi - 20^o)$], we can determine the phasing at which the pattern will be omnidirectional.

For A/B = 1.2, $\theta = 100^o$, and $\phi = 45^o$ and 225^o,

$$\frac{k_1}{k_2} \sim 0.676 \, |\sin(\psi - 20^o) - \cos(\psi - 20^o)| \quad , \tag{19}$$

while for $\phi = 135^o$ and 315^o,

$$\frac{k_1}{k_2} \sim 0.965 \, |\sin(\psi - 20^o) + \cos(\psi - 20^o)| \quad . \tag{20}$$

Equations (19) and (20) are plotted versus ψ in figure 12, along with our empirically determined value of k_1/k_2. Note that the only phasing where all three functions of k_1/k_2 are equal is at $\psi = 300^o$. Therefore, the pattern must be omnidirectional at this phasing. Referring to figure 10, we see that this is the case.

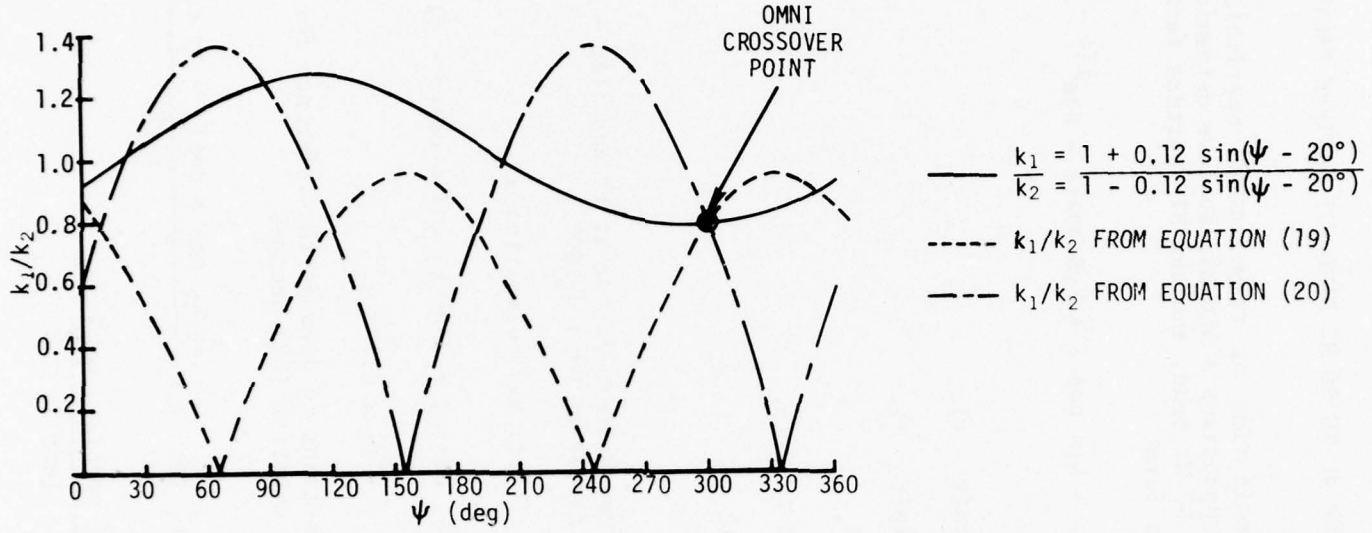

Figure 12. 70 to 80 Hz Band Determination of Omnidirectional Pattern Phasing Angle

NEW 40 TO 50 HZ BAND WTF PATTERN FACTOR

Based on a combination of very limited nearfield and farfield measurements (see appendixes A and B), we have determined empirically that, in the 40 to 50 Hz band, the new WTF pattern factor for the H_ϕ component is of the form

$$F(\phi) \sim k_1 A \cos\phi + k_2 B \cos(\phi - \theta) e^{j(\psi - \tau)} \quad , \tag{21}$$

where

$k_1 = 1 + X_1 \sin(\psi - \tau)$,

$k_2 = 1 - X_2 \sin(\psi - \tau)$,

$\tau = 20^o$ to 30^o,

$X_1 \sim X_2 \sim 0.10$ to 0.15,

$A/B = 1.30$, and

$\theta = 107^o$.

Note that the new pattern factor at τ^o and $(180 + \tau)^o$ is identical to the old pattern factor at 0^o and 180^o.

The magnitude of $F(\phi)$ may be written as

$$|F(\phi)| \sim [k_1^2 A^2 \cos^2\phi + 2AB k_1 k_2 \cos\phi \cos(\phi - \theta) \cos(\psi - \tau) + k_2^2 B^2 \cos^2(\phi - \theta)]^{\frac{1}{2}} \quad . \tag{22}$$

If the WTF EW antenna is used as the reference for defining the new WTF pattern factor, equation (22) becomes

$$\left|\frac{F(\phi)}{B}\right| \sim \frac{A}{B}\left\{k_1^2 \cos^2\phi + \frac{2k_1 k_2 \cos\phi \cos(\phi - \theta) \cos(\psi - \tau)}{(A/B)} + \frac{k_2^2 \cos^2(\phi - \theta)}{(A/B)^2}\right\}^{\frac{1}{2}} \quad . \tag{23}$$

Referring to equation (23), we see that the maximum field strength produced at any single location is not realized when $\psi = 0^o$ or 180^o. Furthermore, the field strengths received at 60^o and 300^o phasing will not be identical.

When $(\phi - \theta) \sim \pi/2$ or $3\pi/2$,

$$\left|\frac{F(\phi)}{B}\right| \sim k_1 \frac{A}{B} \cos\phi = [1 + X_1 \sin(\psi - \tau)]\left(\frac{A}{B}\right)\cos\phi \; ; \qquad (24)$$

and when $\phi \sim \pi/2$ or $3\pi/2$,

$$\left|\frac{F(\phi)}{B}\right| \sim k_2 \cos(\phi - \theta) = [1 - X_2 \sin(\psi - \tau)]\cos(\phi - \theta) \; . \qquad (25)$$

Thus, in the 40 to 50 Hz band, the field strengths received at azimuth angles of $\pi/2$ or $3\pi/2$ are not independent of the WTF phasing angle ψ.

The 45^o and 315^o phasing WTF pattern factors are presented in figure 13, while a comparison of the Stumpneck and Tromsö measured and predicted WTF pattern factors is presented in figures 14 and 15. For all three of these figures, $\tau = 30^o$, $k_1 = 1 + 0.15 \sin(\psi - 30^o)$, and $k_2 = 1 - 0.15 \sin(\psi - 30^o)$.

From figure 13, we see that 315^o phasing yields an omnidirectional pattern (i.e., $F(\phi)/B = 0.7 \pm 0.2$ dB at all bearings) and that 45^o phasing does not equal 315^o phasing except at the $\Delta = 0^o$ bearings (0^o, 80^o, 180^o, and 260^o). At Swansboro, 315^o phasing yields ~13 dB greater field strengths than does 45^o phasing, while at Tromsö, 45^o phasing produces 2 dB higher field strengths than 315^o phasing.

The measured data presented in figures 14 and 15 were taken by NRL in 1974 and 1975 during nighttime propagation conditions.[5] Field strengths were measured at some phasings (0^o and 180^o) during many nights; also, field strengths at other phasings (60^o and 300^o) were measured during only 2 to 4 nights. Since ELF nighttime propagation is much more variable than daytime propagation,[6] the average measured data at each phasing presented in figures 14 and 15 should be interpreted with caution.

The solid-line curve in figures 14 and 15 is calculated from the old WTF pattern factor (equation (5)), and the dashed-line curve is calculated from the new WTF pattern factor (equation (23)). From these figures, we see that equation (23) is a good approximation of the Stumpneck and Tromsö measured pattern factors.

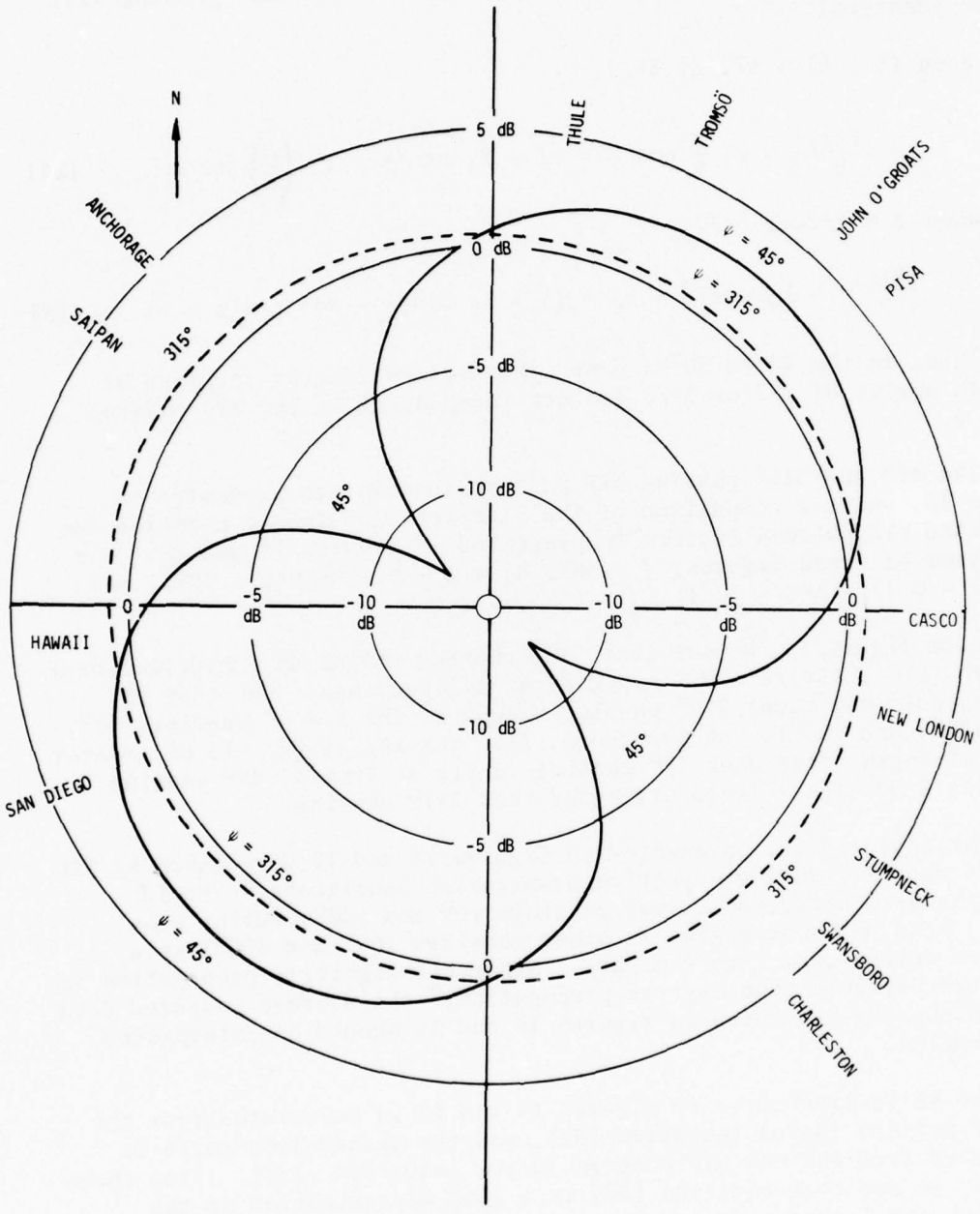

Figure 13, 40 to 50 Hz Band New WTF Pattern Factor Versus Receiving Location Bearing; ψ = 45° and 315°

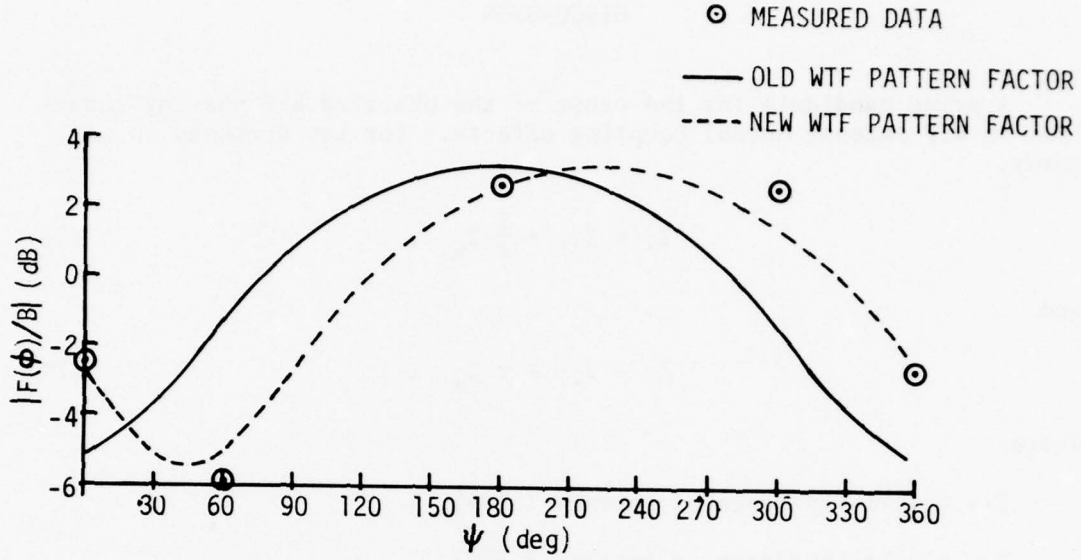

Figure 14. 42 Hz Comparison of Measured Nighttime Data With WTF Pattern Factors for Stumpneck, Maryland (0 dB = -147.8 dBA/m, $\Delta \sim 45^{\circ}$)

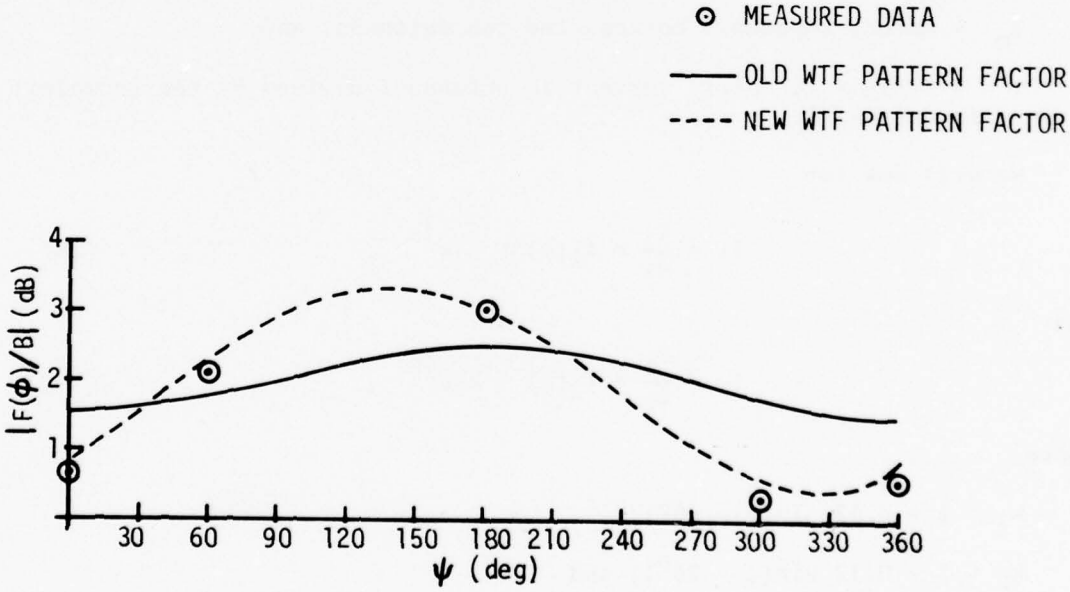

Figure 15. 42 Hz Comparison of Measured Nighttime Data With WTF Pattern Factors for Tromsö, Norway (0 dB = -159.5 dBA/m, $\Delta \sim -45^{\circ}$)

DISCUSSION

A prime candidate for the cause of the observed WTF phasing anomalies is WTF antenna mutual coupling effects. For two antennas in an array,

$$Z_1 = Z_{11} + \frac{1}{r} Z_m \quad , \tag{26}$$

and

$$Z_2 = Z_{22} + r\, Z_m \quad , \tag{27}$$

where

Z_{11} = self-impedance of antenna 1 (NS),

Z_{22} = self-impedance of antenna 2 (EW),

Z_1 = terminal impedance of antenna 1,

Z_2 = terminal impedance of antenna 2,

Z_m = mutual impedance between the two antennas, and

$r = I_1/I_2$ = (complex) current in antenna 1 divided by the (complex) current in antenna 2.

We will now let

$$I_1 = \frac{V_1}{Z_1} = f_1(\psi) \sim k_1 e^{j\alpha} \quad , \tag{28}$$

and

$$I_2 = \frac{V_2}{Z_2} = f_2(\psi) \sim k_2 e^{j\beta} \quad , \tag{29}$$

where

$k_1 \sim 1 + 0.12 \sin(\psi - 20^o)$,

$k_2 \sim 1 - 0.12 \sin(\psi - 20^o)$, and

V_1 and V_2, respectively, are the terminal voltages of antennas 1 and 2.

Thus, the WTF pattern factor may be expressed as

$$F(\phi) \sim k_1 A \cos\phi\, e^{j\alpha} + k_2 B \cos(\phi - \theta) e^{j\beta} e^{j\psi} \quad . \tag{30}$$

The magnitude of $F(\phi)$ may be written as

$$\begin{aligned} |F(\phi)| &\sim |k_1 A \cos\phi + k_2 \beta \cos(\phi - \theta) e^{j(\psi - (\alpha - \beta))}| \\ &\sim \left[k_1^2 A^2 \cos^2\phi + 2k_1 k_2 AB \cos\phi \cos(\phi - \theta) \cos(\psi - (\alpha - \beta)) \right. \\ &\quad \left. + k_2^2 B^2 \cos^2(\phi - \theta)\right]^{\frac{1}{2}} \end{aligned} \tag{31}$$

If $\alpha - \beta = 20^\circ$, equation (31) reduces to equation (9). Therefore, it appears that the WTF phasing anomalies are caused by mutual coupling effects (due to parasitics or circuit set up). It is interesting to note that no WTF phase anomalies were observed until about a year after the WTF NS buried antenna was installed.

CONCLUSIONS

Based upon a combination of nearfield and farfield measurements, a new empirical WTF pattern factor has been determined that quantitatively explains those WTF phasing anomalies that have been observed since 1974. Among the anomalies explained are

1. ψ° phasing does not equal $(360 - \psi)^\circ$ phasing, contrary to the normal behavior of crossed dipoles;

2. the maximum field strength at any single receiving location is not when $\psi = 0$ or 180°;

3. the 70 to 80 Hz H_ϕ field strengths received in New London (which is broadside to the WTF NS antenna) and Tromsö (which is broadside to the WTF EW antenna) are no longer independent of the phasing angle ψ;

4. the WTF antenna phasing shift appears to be -20° to -30°;

5. the WTF antenna effective dipole moment does not appear to be independent of ψ; and

6. the WTF antenna phasing shift appears to be a function of receiving location (i.e., azimuth angle).

It appears that the WTF phasing anomalies are caused by WTF antenna mutual coupling effects (due to parasitics or circuit set up).

REFERENCES

1. P. R. Bannister, F. J. Williams, A. L. Dahlvig, and W. A. Kraimer, Wisconsin Test Facility Transmitting Antenna Pattern and Steering Measurements, NUSC Technical Report 4395, 13 March 1973.

2. P. R. Bannister, F. J. Williams, A. L. Dahlvig, and W. A. Kraimer, "Wisconsin Test Facility Transmitting Antenna Pattern and Steering Measurements," IEEE Transactions on Communications, vol. COM-22, no. 4, 1974, pp. 412-418.

3. P. R. Bannister and F. J. Williams, "Results of the August 1972 Wisconsin Test Facility Effective Earth Conductivity Measurements," Journal of Geophysical Research, vol. 79, no. 4, 10 February 1974, pp. 725-732 (corrections listed on p. 2698 of vol. 79, no. 17, 10 June 1974).

4. J. R. Dinger, private communication.

5. J. R. Davis, private communication.

6. P. R. Bannister, "Variations in Extremely Low Frequency Propagation Parameters," Journal of Atmospheric and Terrestrial Physics, vol. 37, no. 9, 1975, pp. 1203-1210.

Appendix A

HISTORY OF WTF PHASING TESTS AND ANOMALIES

1. August 1971, Naval Underwater Systems Center (NUSC) 300 km Pattern Test. Wisconsin Test Facility (WTF) NS and EW antennas were excited separately at 45 and 75 Hz.

2. September 3, 1971, NUSC 300 km Phasing Test. 45 and 75 Hz field strengths were measured at two sites with antenna phasings of 0°, 90°, 180°, and 270°.

3. September 20 to 24, 1971, NUSC 1.7 Mm Phasing Test. 45 and 75 Hz field strengths were measured at two farfield sites with antenna phasings of 0°, 60°, 80°, 120°, and 180°.

4. October/November 1971, Joint NUSC/MITLL (Massachusetts Institute of Technology, Lincoln Laboratories) Farfield Propagation Tests. Field strengths were measured at 41 to 49 and 71 to 79 Hz, with a WTF antenna phasing of 60°.

5. May 1972, Joint NUSC/MITLL Farfield Propagation Tests. Field strengths were measured at 41 to 49 and 71 to 79 Hz, with a WTF antenna phasing of 120°.

6. August 1972, NUSC 50 km WTF Effective Conductivity Measurements. Each WTF antenna was excited separately at 45 and 75 Hz. Results for A/B (ratio of NS to EW antenna effective dipole moment) and pattern of individual antennas were identical to the August/September 1971 pattern and phasing test results.

7. March/April 1973, NUSC 50 km 76 Hz Comparison of Buried and Elevated WTF NS Antennas. Results were identical to the August 1972 results.

8. July 1973, NUSC 50 km Measurements. Results were also identical to the previous results.

9. 1972 to 1974, NUSC 42 and 76 Hz Measurements in Connecticut at 0° and 180° phasing. Only one apparent phasing anomaly was observed (see item 12).

10. Summer and fall 1974, NUSC Conductivity Measurements in the Western States Using the WTF as the Source (0° Phasing). No phasing anomalies were observed.

11. March 13 to 17, 1974, First Phasing Anomaly Observed. The 42 Hz 60° field strengths measured in Maryland (by NRL) were ∿8 dB lower than predicted. Simultaneous measurements in Connecticut (NUSC) and Norway (NRL) indicated little change in field strength. However, it was later learned that the real-time integrator in Maryland was improperly adjusted and that the observed discrepancy was only about 4 dB.

12. July/August/September 1974, NUSC 76 Hz 0° Phasing Measurements in Connecticut. These measurements were ∿1 dB higher than at 180° phasing (the expected difference is 0.1 dB).

13. November 5 to 6, 1974, NRL 60° Phasing Measurements in Maryland. These measurements were ∿4 dB lower than expected, while the 300° phasing measurements were ∿4 dB higher than expected.

14. December 1974, NRL 300° Phasing Measurements in Norway. These measurements were ∿3 dB lower than predicted (as well as previously measured) values. Since the Norway site is directly broadside to the WTF EW antenna, the received field strength should be independent of phasing angle ψ (i.e., only the WTF NS antenna is received).

15. January 1975, NRL 180° Phasing Measurements in Norway. These measurements were the same as previously observed.

16. February 11 to 13, 1975, NRL 60° Phasing Measurements in Maryland. These measurements were ∿4.5 dB lower than expected, while the 300° phasing measurements were ∿4.5 dB higher than expected (i.e., these measurements are consistent with the November 5 to 6, 1974 results). In Greenland, the 0° phasing results were about as expected, while the 60° and 300° phasing results were lower than expected (by ∿3 and 7 dB, respectively).

17. March 1975, NRL 42 Hz 0° Phasing Measurements in Greenland, Norway, and Italy. These measurements were 1 to 3 dB lower than predicted.

18. May 1975, Simultaneous 76 Hz NUSC/NRL Measurements in North Carolina, Maryland, and Greenland. These measurements indicated that 300° does not equal 60° and 120° does not equal 240° phasing. In North Carolina, the May 1975 60° field strengths were ∿3 dB lower than that measured in September 1971, while the 120° field strengths were ∿1 dB lower. The May 1975 300° field strengths were approximately the same as the September 1971 80° field strengths.

19. July/August 1975, NRL 76 Hz 0° Phasing Measurements in Greenland, Norway, and Italy. These measurements were approximately 2 dB lower than predicted, while the Connecticut (NUSC) measurements were the same as previously measured. Also, NRL NS antenna measurements at the same sites were lower than predicted.

20. July/August 1975, NUSC 76 Hz 50 km Measurements. The single antenna measurements (at a few selected sites) were identical (in both effective dipole moment and pattern) to previous NUSC measurements. At all the 35 sites measured, 0° phasing was not 0° (i.e., if the phasing were really 0°, a null should be observed at some receiving angle; however, no null was observed at any site). At all the 35 sites, 0° phasing looked more like -20° phasing. Also, during this period, 60° and 300° phasings were measured at 18 sites. The 60° and 300° field strengths were not identical at any of the 18 sites.

21. September 15 to 19, 1975, NUSC 76 Hz Daytime Connecticut Measurements at 60° and 300° Phasings. These measurements were not the same (the 300° field strengths were ∿1.6 dB higher). Since the WTF EW antenna is the only (±0.1 dB) contributor to the Connecticut field strength in the H_ϕ direction (i.e., the Connecticut site is practically broadside to the WTF NS antenna), the dipole moment of the EW antenna must have been increased at 300° phasing and decreased at 60° phasing. Also, during this time, the 300° phasing field strengths were ∿4.5 dB higher than the 60° phasing field strengths in Maryland and about the same in Greenland.

22. September/October/November 1975, the Connecticut Nighttime Field Strengths Measured in September (300° Phasing). These measurements were ∿1 dB higher than those measured in October and November (0° phasing).

23. October/November 1975, The 0° Field Strengths Measured in Greenland and Norway. These measurements were ∿2 dB lower than predicted, while the measurements in Connecticut, Maryland, and Italy were the same or higher.

24. March/April 1976, The 0° Field Strengths Measured in Greenland, Norway, and Italy. These measurements were ∿2 dB lower than predicted.

25. October 1975, NUSC 42 and 76 Hz Measurements at Three Sites (∿50 km) at 15 Different Phasings. Four different interpretations of these measurements resulted in the same conclusions: (1) the WTF antenna phasing shift is -20° to -30° (i.e., when the antennas are set up at 60° phasing, the actual phasing is 30° to 40°); (2) the effective WTF dipole moment is not constant with phasing angle; and (3) the WTF antenna phasing shift appears to be a function of azimuth angle. At one of these sites, a relative phase measurement (with respect to a stable source) was made. It showed that the NS antenna lagged the EW antenna by ∿25°.

26. July and October 1975, Measurements at the WTF Transmitting Station by Illinois Institute of Technology Research Institute (IITRI) and NUSC of the Antenna Current Magnitude and Relative Phase Between Antennas. No phasing anomalies were noted.

27. August 1976, Farfield Verification Test of the New WTF Pattern Factor. Measurements were taken by NUSC in Connecticut and Maine and by NRL in Maryland and Norway at approximately every 30° phasing, as well as on the individual WTF antennas. The new WTF pattern factor was in excellent agreement with the measured data.

Appendix B

SUMMARY OF NEARFIELD MEASUREMENTS

During July/August 1975, we made 76 Hz measurements at about thirty-five 50 km sites. The single antenna (i.e., NS or EW) measurements (at a few selected sites) were identical (in both effective dipole moment and pattern) to our previous measurements. At all 35 sites measured, 0° phasing was not 0°. That is, if the phasing were really 0°, a null should be observed at some receiving angle. No null was observed at any site. The 0° phasing looked more like -20° phasing at all 35 sites. Also, during this period, 60° and 300° phasings were measured at 18 sites. The 60° and 300° field strengths were not identical at any of the 18 sites.

In October 1975, we made 42 and 76 Hz measurements at three sites for 15 different Wisconsin Test Facility (WTF) phasing angles (see figure B-1). The sites were Mile 403, at Barnes, and at Ashland and Seeley, all in Wisconsin. Four different interpretations of these measurements resulted in the same conclusions:

1. $\psi°$ phasing does not equal $360° - \psi°$ phasing;

2. the WTF antenna phasing shift appears to be -20° to -30°;

3. the effective WTF dipole moment is not constant with phasing angle; and

4. the WTF phasing shift appears to be a function of azimuth angle.

At one of the sites (Mile 403), a relative phase measurement (with respect to a stable source) was made. It showed that the NS antenna lagged the EW antenna by approximately 25°.

For a particular receiving site, the total horizontal magnetic field strength produced by each WTF antenna (when energized separately) will have a maximum value at some angle with respect to true north. Referring to figure B-2, we see that when the WTF antennas are operated at a particular phasing, the received field strength (H_θ) as a function of the receiving orientation with respect to true north (θ) may be expressed as

$$H_\theta = a \cos(\theta - \alpha) + b \cos(\theta - \beta)e^{j\psi} = C_{NS} + C_{EW}e^{j\psi} \quad . \qquad \text{(B-1)}$$

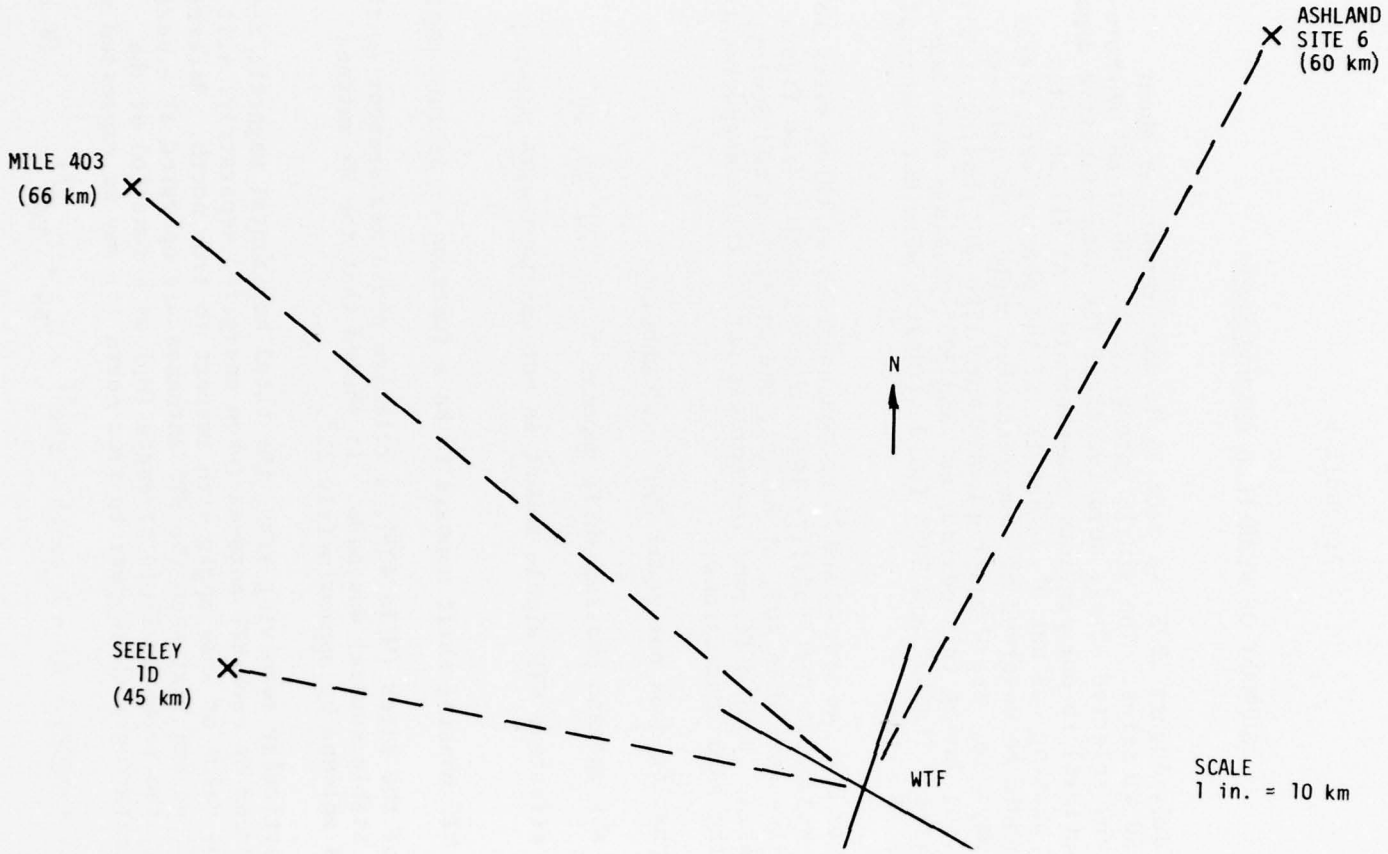

Figure B-1. October 1975 Nearfield WTF Phasing Anomaly Test Measurement Locations

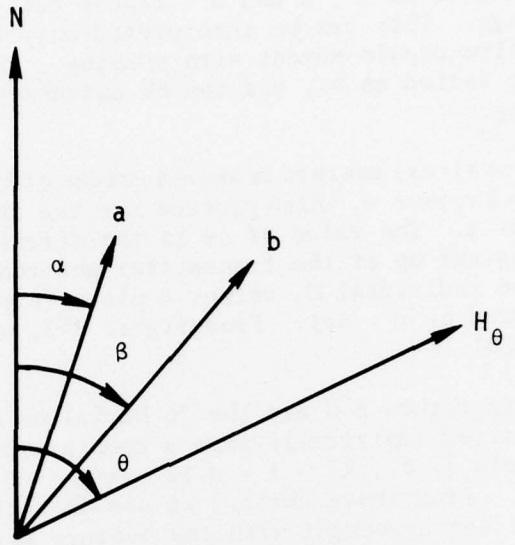

Figure B-2. Diagram Employed for Calculation of Received Field Strength as a Function of Receiving Antenna Orientation

The magnitude of H_θ is

$$|H_\theta| = \left[C_{NS}^2 + C_{EW}^2 + 2C_{NS}C_{EW} \cos \psi\right]^{\frac{1}{2}} , \qquad \text{(B-2)}$$

and the angle at which the received field strength is maximum (θ_{max}) is

$$\theta_{max} = \tfrac{1}{2} \tan^{-1}\left\{\frac{a^2 \sin 2\alpha + b^2 \sin 2\beta + 2ab \cos \psi \sin(\alpha + \beta)}{a^2 \cos 2\alpha + b^2 \cos 2\beta + 2ab \cos \psi \cos(\alpha + \beta)}\right\} . \qquad \text{(B-3)}$$

When $\theta - \beta = \pm n\pi/2$ (n odd) ,

$$H_\theta = a \cos(\theta - \alpha) , \qquad \text{(B-4)}$$

and when $\theta - \alpha = \pm n\pi/2$ (n odd) ,

$$H_\theta = b \cos(\theta - \beta) . \qquad \text{(B-5)}$$

That is, when $\theta - \beta = \pm n\pi/2$, there will be no contribution from the WTF EW antenna. Likewise, when $\theta - \alpha = \pm n\pi/2$, there will be no contribution from the WTF NS antenna. At these two receiving angles, the received field strengths will not depend upon the WTF antenna phasing if the WTF effective dipole moment is constant with phasing angle.

At both frequencies and at all three sites, the H_θ field strengths at the receiving angles of $\theta - \alpha$ and $\theta - \beta$ were not constant at different WTF antenna phasings. This can be interpreted only as a change in the WTF antenna effective dipole moment with phasing. The NS antenna effective dipole moment varied as k_1, and the EW antenna effective dipole moment varied as k_2.

The 76 Hz (three sites) average measured values of k_1, k_2, and k_1/k_2 are plotted in figure B-3 versus ψ. Also plotted are the three site average values of $\Delta\psi$ versus ψ. The value of $\Delta\psi$ is the difference between the WTF antenna phasing set up at the transmitter and the apparent phasing determined from the individual H_θ versus θ plots (employing equation (B-2), with ψ replaced by $\psi + \Delta\psi$). From figure B-3, we see that the average $\Delta\psi$ is $\sim -20°$.

Also plotted in figure B-3 are the 76 Hz values of k_1, k_2, and k_1/k_2 that were derived empirically from a combination of nearfield and farfield measurements [i.e., $k_1 \sim 1 + 0.12 \sin(\psi - 20°)$ and $k_2 \sim 1 - 0.12 \sin(\psi - 20°)$]. From these curves, we see that the k_2 empirical formula is in excellent agreement with the average measured nearfield values, while the k_1 and k_1/k_2 empirical formulas are in fairly good agreement with the average measured nearfield values. However, it should be remembered that the nearfield averages were determined from data taken at only three sites.

A comparison of the measured and predicted values of the 76 Hz H_{max} component as a function of ψ is presented in figures B-4 and B-5. The solid-line curve in each figure is calculated (from equations (B-2) and (B-3) under the assumption that $k_1 = k_2 = 1$ (i.e., no WTF effective dipole moment change). The dotted-line curve is calculated from equations (B-2) and (B-3), with "a" replaced by $k_1 a$, "b" replaced by $k_2 b$, and ψ replaced by $\psi - 20°$, using the empirically determined values of k_1 and k_2.

From these figures, we see that at all three sites the calculated values (employing the empirically determined values of k_1 and k_2) of H_{max} are in excellent agreement with the H_{max} measured values.

The 42 Hz nearfield measurements were somewhat confusing in that some interpretations indicated a -20° to -25° WTF phasing shift; other interpretations yielded a WTF phasing shift of -25° to -30°. Based upon the very limited measurements taken to date, it appears that

$$k_1 \sim 1 + X_1 \sin(\psi - \tau) \quad ,$$

$$k_2 \sim 1 - X_2 \sin(\psi - \tau) \quad ,$$

$$\tau = 20° \text{ to } 30° \quad , \text{ and}$$

$$X_1 \sim X_2 \sim 0.10 \text{ to } 0,15 \quad .$$

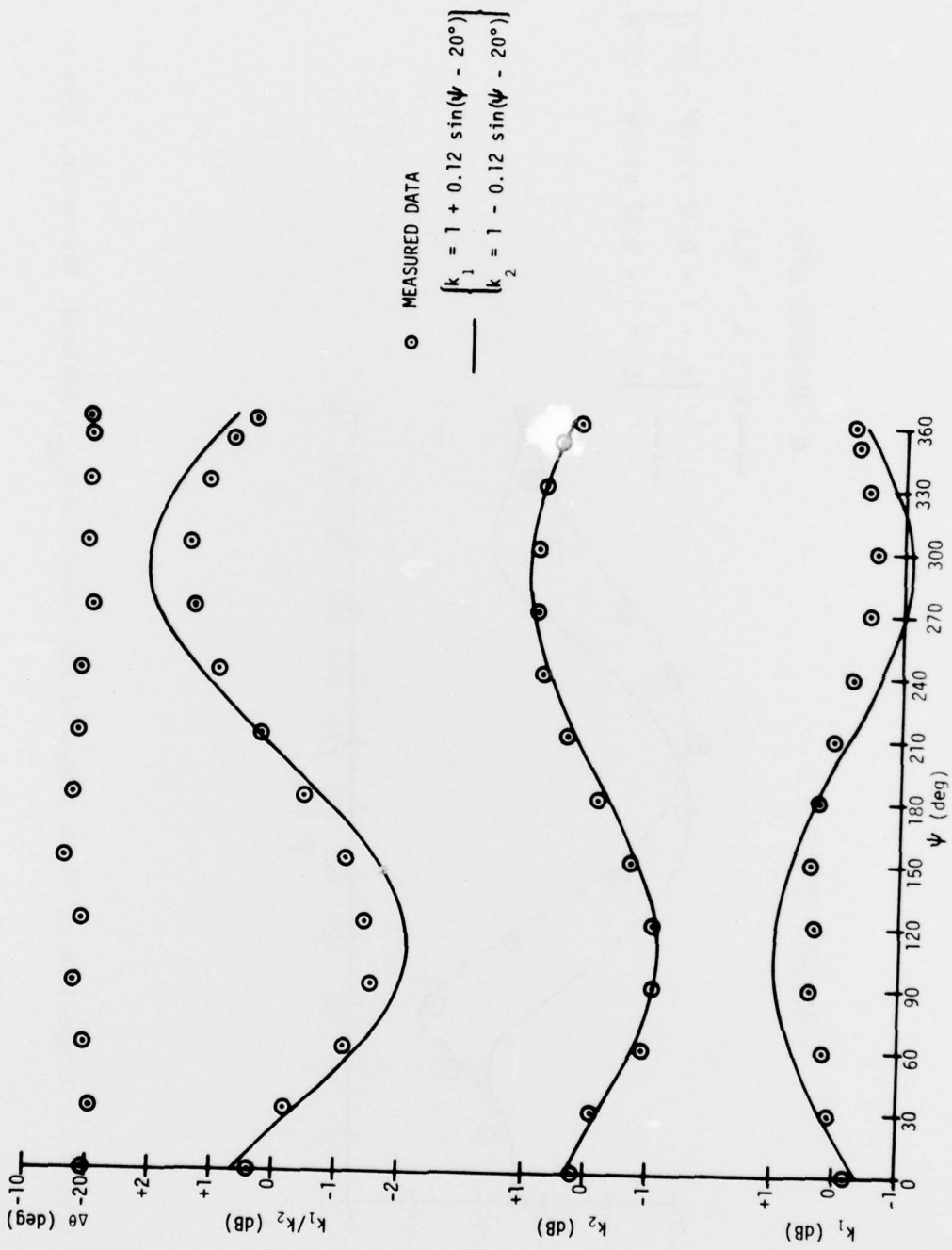

Figure B-3. Plots of k_1, k_2, k_1/k_2, and $\Delta\psi$ Versus ψ for f = 76 Hz

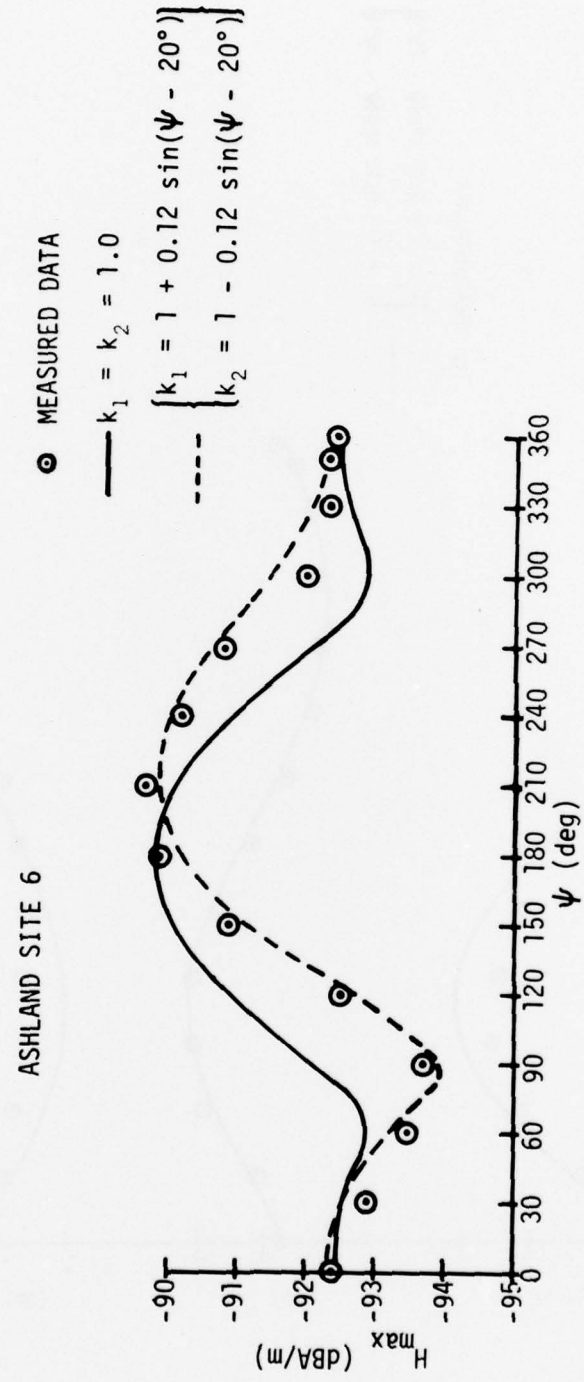

Figure B-4. Comparison of 76 Hz Measured and Predicted H_{max}, Ashland, Wisconsin, Site 6

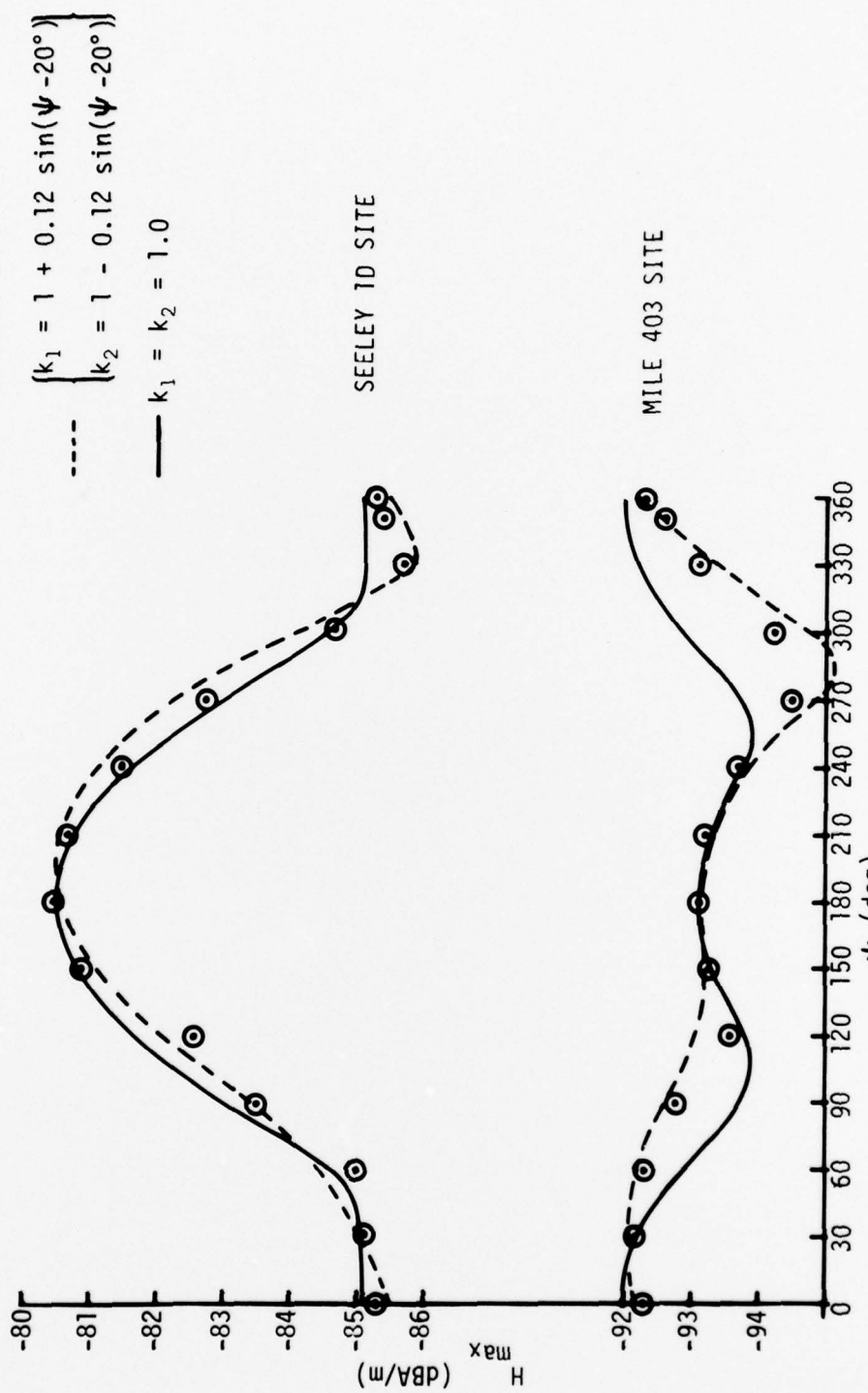

Figure B-5. Comparison of Measured and Predicted H_{max}, Seeley, Wisconsin, 1D and Mile 403 Sites

INITIAL DISTRIBUTION LIST

Addressee	No. of Copies
ONR, Code 427, 485, 412-8, 480, 410, Earth Sciences Division (T. Quinn))	6
ONR Branch Office, Chicago (F. L. Dowling)	1
NRL, (J. Davis, W. Meyers, R. Dinger, F. Kelly), Code 6451 (D. Forester), 6454 (J. Clement, E. Compy, P. Lubitz, J. Schelleng)	9
NAVELECSYSCOMHQ, Code 03, PME-117, -117-21, -117-213, -117-213A, -117-215	6
NELC, (R. Moler, H. Hughes, R. Pappert, Code 3300)	4
NAVMAT, Code PM2-00 (RADM J. Metzel, Jr.), PM2-001 (J. Crone)	2
NAVSEASYSCOMHQ, Code SEA-03424 (W. Welsh), -0227 (J. Fox), -03C, -034, -06H, -660C, -660D, PMS-396	8
DTNSRDC/A, Code 2782 (W. Andahazy, L. Dadin, D. Everstine, B. Hood, D. Nixon, D. Peoples, T. Shaw, F. Walker), 2732 (F. Baker, D. Fairhead), 2813 (E. Bieberich), 278 (H. Boroson), 2733 (P. Field, D. Rockwell), 0700 (R. Robinson)	15
DTNSRDC/C, Code 1548 (R. Knutson), 1102.2 (J. Stinson)	2
NAVSURFWPNCEN, Code WE-04 (W. Stoll, D. Norton), -12 (K. Bishop, M. Lackey, Jr., W. Menzel, J. Miller, E. Peizer, R. Stabnow, G. Stimak, J. Whelan), WR-43 (R. Brown, J. Cunningham, Jr., M. Kraichman, G. Usher)	14
NAVCOASTSYSLAB, Code 721 (C. Stewart), 773 (K. Allen), 792 (M. Wynn, W. Wynn)	4
NAVSEC, Code 6157 B (C. Butler, G. Kahler, D. Muegge)	3
NAVFACENGSYSCOM, Code FPO-1C (W. Sherwood), -1C7 (R. McIntyre, A. Sutherland)	3
NAVAIR, Code AIR-0632 B (L. Goertzen)	1
NAVAIRDEVCEN, Code 2022 (J. Duke, R. Gasser, E. Greeley, A. Ochadlick, L. Ott, W. Payton, W. Schmidt)	7
NAVSHIPYD PTSMH, Code 280 (B. Murdock)	1
AFWTF, Code 01A (CDR W. Danner), 32 (LT R. Elston), 412 (P. Burton, R. Kirkpatrick)	4
NISC, Code 20 (G. Batts), 43 (J. Erdmann), OW17 (M. Koontz)	3
NOSC, Code 407 (C. Ramstedt)	1
NAVPGSCOL, Code 06 (R. Fossum)	1
U. S. Naval Academy, Anna. (C. Schneider)	1
CNO, Code OP-02, 03EG, -090, -23, -902, 941, -942U, 201, -953, -954, -96	11
CNM, Code MAT-00, -03L, -0302, -034, -03T (CAPT Walker), ASW-23	6
SUBASE LANT	1

INITIAL DISTRIBUTION LIST (Cont'd)

Addressee	No. of Copies
NAVSUBSUPFACNLON	1
NAVWPNSCEN	1
NAVSUBTRACENPAC	1
CIVENGRLAB	1
NAVSUBSCOL	1
NAVWARCOL	1
DDC, Alexandria	12
Engineering Societies Library United Engineering Center 345 East 47th St. New York, NY 10017	1
GTE Sylvania (G. Pucillo, D. Esten, R. Warshamer, D. Boots, R. Row) Needham, MA 02194	5
Lockheed (J. Reagan, W. Imhof, T. Larsen) Palo Alto, CA 94302	3
Lawrence Livermore Labs (J. Lytle, E. Miller) Livermore, CA 94550	2
Ratheon Co. (J. de Bettencourt) Norwood, MA 02062	1
Univ. of Nebraska Dept. of EE (E. Bahar) Lincoln, NB 68508	1
NOAA (D. Barrick, R. Fitzgerrell, D. Grubb, J. Wait (ERL)) U.S. Dept. of Commerce Boulder, CO 80302	4
Newmont Exploration Ltd. (A. Brant) Danbury, CT 06810	1

INITIAL DISTRIBUTION LIST (Cont'd)

Addressee	No. of Copies
IITRI (J. Bridges) Chicago, IL 60068	1
Stanford Univ. Dept. of EE (F. Crawford) Stanford, CA 94305	1
Stanford Univ. P.O. Box 7457 (J. Wikswo) Menlo Park, CA 94025	1
Univ. of Colorado Dept. of EE (D. Chang) Boulder, CO 80302	1
SRI (L. Dolphin, Jr., A. Fraser-Smith, J. Chown, R. Honey, M. Morgan) Menlo Park, CA 94025	5
Air Force Cambridge Research Lab (R. Fante) Bedford, MA 01730	1
USGS - Federal Centre Regional Geophysics Branch (F. Frischknecht) Denver, CO 80225	1
Colorado School of Mines Geophysics Dept. (R. Geyer, G. Keller) Golden, CO 80401	2
Univ. of Arizona Dept. of Mining & Geological Engineering (D. Hastings) Tuscon, AZ 85721	1
Univ. of Michigan Radiation Lab (R. Hiatt) Ann Arbor, MI 48105	1

INITIAL DISTRIBUTION LIST (Cont'd)

Addressee	No. of Copies
U. S. Army Cold Regions Research & Eng. Lab (P. Hoekstra) Hanover, NH 03755	1
Univ. of Washington Dept. of EE (A. Ishimaru) Seattle, WA 98105	1
Univ. of Wisconsin Dept. of EE (R. King) Madison, WI 53706	1
Univ. of Wyoming Dept. of EE (J. Lindsay, Jr.) Laramie, WY 82070	1
Univ. of Arizona College of Earth Sciences (L. Lepley) Tucson, AZ 85719	1
Univ. of Illinois Dept. of EE (R. Mittra) Urbana, IL 61801	1
Univ. of Kansas (R. Moore) Lawrence, KS 66044	1
Washington State Univ. Dept. of EE (R. Olsen) Pullman, WA 99163	1
Institute for Telecommunication Services U.S. Dept. of Commerce (R. Ott) Boulder, CO 80302	1
North Carolina State Univ. Dept. of EE (R. Rhodes) Raleigh, NC 27607	1

INITIAL DISTRIBUTION LIST (Cont'd)

Addressee	No. of Copies
Ohio State Univ. Dept. of EE (J. Richmond) Columbus, OH 43212	1
MIT Lincoln Laboratory (J. Ruze, D. White, J. Evans, A. Griffiths, L. Ricardi) Lexington, MA 02137	5
Univ. of Utah Dept. of Geological & Geophysical Sciences (S. Ward) Salt Lake City, UT 84112	1
Purdue Univ. School of EE (W. Weeks) Lafayette, IN 47907	1
Nat'l Oceanographic & Atmospheric Admin. Wave Propagation Lab (G. Little) Boulder, CO 80302	1
Univ. of Pennsylvania Moore School of EE D2 (R. Showers) Philadelphia, PA 19174	1
Dynatrend Incorporated (F. Ostherr, L. Parente) Burlington, MA 01803	2
Dynatrend Incorporated/DC (E. Mansfield) Arlington, VA 22209	1
Cadcom Incorporated (D. Brake, W. Hicks, F. Klappenberger, N. Nicholas) Annapolis, MD 21401	4
Electric Boat Division (R. Clark, L. Conklin, H. Hemond, G. McCue, D. Odryna) Groton, CT 06340	5

INITIAL DISTRIBUTION LIST (Cont'd)

Addressee	No. of Copies
Science Application Incorporated (J. Czika) McLean, VA 22101	1
JHU/APL (W. Chambers, P. Gueschel, L. Hart, H. Ko) Silver Spring, MD 20910	4